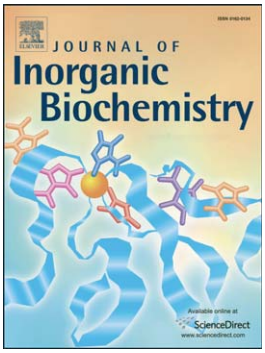

Silver(I) complexes with phthalazine and quinazoline as effective agents against pathogenic *Pseudomonas aeruginosa* strains

Biljana . Glišić, Lidija Senerovic, Peter Comba, Hubert Wadepohl, Aleksandar Veselinovic, Dušan R. Milivojevic, Miloš I. Djuran, Jasmina Nikodinovic-Runic

PII: S0162-0134(15)30127-6
DOI: doi: 10.1016/j.jinorgbio.2015.11.026
Reference: JIB 9857

To appear in: *Journal of Inorganic Biochemistry*

Received date: 1 September 2015
Revised date: 20 November 2015
Accepted date: 30 November 2015

Please cite this article as: Biljana . Glišić, Lidija Senerovic, Peter Comba, Hubert Wadepohl, Aleksandar Veselinovic, Dušan R. Milivojevic, Miloš I. Djuran, Jasmina Nikodinovic-Runic, Silver(I) complexes with phthalazine and quinazoline as effective agents against pathogenic *Pseudomonas aeruginosa* strains, *Journal of Inorganic Biochemistry* (2015), doi: 10.1016/j.jinorgbio.2015.11.026

Ms. No. JIB-15-0901 (2nd revised version)

Silver(I) complexes with phthalazine and quinazoline as effective agents against pathogenic *Pseudomonas aeruginosa* strains

Biljana Đ. Glišić[a,#], Lidija Senerovic[b,#], Peter Comba[c,*], Hubert Wadepohl [c], Aleksandar Veselinovic[d], Dušan R. Milivojevic[b], Miloš I. Djuran[a,*], Jasmina Nikodinovic-Runic[b,*]

[a]*Department of Chemistry, Faculty of Science, University of Kragujevac, R. Domanovića 12, PO Box 60, 34000 Kragujevac, Serbia*

[b]*Institute of Molecular Genetics and Genetic Engineering, University of Belgrade, Vojvode Stepe 444a, 11000 Belgrade, Serbia*

[c]*Anorganisch-Chemisches Institüt and Interdisciplinary Center for Scientific Computing (IWR), University of Heidelberg, Im Neuenheimer Feld 270, 69120 Heidelberg, Germany*

[d]*Faculty of Medicine, Department of Chemistry, University of Niš, 18000 Niš, Serbia*

[#]B.Đ.G and L.S. contributed equally.

[*]Corresponding authors. Tel.: +49 6221 54-8453; fax: +49 6221 54-6617 (P. Comba); Tel.: +381 34 300 251; fax: +381 34 335 040 (M. I. Djuran); Tel.: +381 11 397 6034; fax: +381 11 397 5808 (J. Nikodinovic-Runic).

E-mail address: peter.comba@aci.uni-heidelberg.de (P. Comba); djuran@kg.ac.rs (M. I. Djuran); jasmina.nikodinovic@gmail.com (J. Nikodinovic-Runic).

Abstract

Five silver(I) complexes with aromatic nitrogen-containing heterocycles, phthalazine (phtz) and quinazoline (qz), were synthesized, characterized and analyzed by single-crystal X-ray diffraction analysis. Although different AgX salts reacted with phtz, only dinuclear silver(I) complexes of the general formula $\{[Ag(X\text{-}O)(phtz\text{-}N)]_2(\mu\text{-}phtz\text{-}N,N')_2\}$ were formed, X = NO_3^- **(1)**, $CF_3SO_3^-$ **(2)** and ClO_4^- **(3)**. However, reactions of qz with an equimolar amount of $AgCF_3SO_3$ and $AgBF_4$ resulted in the formation of polynuclear complexes, $\{[Ag(CF_3SO_3\text{-}O)(qz\text{-}N)]_2\}_n$ (**4**) and $\{[Ag(qz\text{-}N)][BF_4]\}_n$ (**5**). Complexes **1-5** were evaluated by in vitro antimicrobial studies against a panel of microbial strains that lead to many skin and soft tissue, respiratory, wound and nosocomial infections. The obtained results indicate that all tested silver(I) complexes have good antibacterial activity with MIC (minimum inhibitory concentration) values in the range from 2.9 to 48.0 μM against the investigated strains. Among the investigated strains, these complexes were particularly efficient against pathogenic *Pseudomonas aeruginosa* (MIC = 2.9 – 29 μM) and had a marked ability to disrupt clinically relevant biofilms of strains with high inherent resistance to antibiotics. On the other hand, their activity against the fungus *Candida albicans* was moderate. In order to determine the therapeutic potential of silver(I) complexes **1**-**5**, their antiproliferative effect on the human lung fibroblastic cell line MRC5, has been also evaluated. Binding of complexes **1**-**5** to the genomic DNA of *P. aeruginosa* was demonstrated by gel electrophoresis techniques and well supported by molecular docking into the DNA minor groove. All investigated complexes showed an improved cytotoxicity profile in comparison to the clinically used $AgNO_3$.

Keywords: Silver(I) complexes; Structural characterization; Antibacterial activity; *Pseudomonas aeruginosa*; Biofilm.

1. Introduction

In the view of the global problem of multi-drug resistant bacterial strains, the search for new antibacterial and antifungal therapeutics is of paramount importance [1,2]. Moreover, the clinical impact of bacterial biofilms as even more resistant forms of bacteria and that of nosocomial (hospital-borne) infections is increasingly recognized [3,4]. Biofilms cause chronic infections in tissues or by developing on the surfaces of medical devices. These infections persist despite inherent and adaptive defense mechanisms of the patient and antibiotic therapy and are characterized by a persisting and progressive pathology, primarily due to the inflammatory response surrounding the biofilm [5]. Therefore, many of these infections are difficult to diagnose and treat efficiently [4,6] and urgently require novel treatment options.

Pseudomonas aeruginosa is a common environmental bacterial species, widely spread in soil and natural water, and is a devious human pathogen, responsible for severe infections. It is a primary cause in infections associated with cystic fibrosis (CF), burn wounds and the use of catheters, and a major cause of nosocomial infections [7-9].The persistence of chronic *P. aeruginosa* lung infections in CF patients is due to the production of a polymer matrix by mucoid strains, forming and growing in the form of biofilms, leading to an increased tolerance to antibiotics and phagocytosis [10-12]. Biofilm formation of *P. aeruginosa* is a wide-spread phenomenon, as members of this species are provided with a large arsenal of cell-associated and secreted virulence factors, which enhance its invasive potential. As a result, they are most commonly encountered in catheter and other medicinal devices [8,12].

Biomedical applications of various transition metal ions and their complexes span anticancer to antimicrobial activity [13-17]. Therefore, metallopharmaceuticals nowadays play a significant role in therapy and diagnosis [15]. Building upon centuries of

accumulated knowledge about antimicrobial properties of silver compounds [18], this element still attracts much interest, specifically also with the new phenomenon of a prolonged anti-bactericidal activity through the so called "zombies" effect, where dead bacteria act as a reservoir of silver ions, which may re-target the living bacteria [19]. Due to higher toxicity for microorganisms and a lower toxicity for mammalian cells, silver(I) compounds were shown to have superior properties in comparison to other metal species with antibacterial activity [20,21]. Importantly, silver(I) compounds have been shown to be active against *P. aeruginosa* biofilms [22].

It is highly desirable for an antimicrobial agent to have long-term effectiveness, to prevent bacterial re-colonization and proliferation, which is characteristic for metal ions such derived from silver and copper that slowly release their cations, trace amounts of which are toxic to bacteria [19,23]. One approach to tune the activity of silver(I) cations is to administer them as complexes [24-27]. Silver(I) sulfadiazine was the first complex used as an antimicrobial agent [28], and ever since many silver(I) complexes have been investigated as antimicrobial agents [25,26]. The success of metallodrugs, in general, is based on the choice of ligands, as these play a crucial role in modifying a specific reactivity, the lipophilicity, in stabilizing specific oxidation states, and suppressing adverse effects of free metal ions [29,30]. It has been suggested that in the case of silver(I) complexes, the most important factors for tuning the biological activity are the type of donor atom and the ease of ligand replacement [31]. Thus, an attractive class of ligands for the synthesis of antimicrobial silver(I) complexes comprises aromatic nitrogen-containing heterocyclic ligands (*N*-heterocycles) [24]. Moreover, these compounds are one of the most important classes of ligands in coordination and bioinorganic chemistry, and have also found use in the rapidly evolving field of metallosupramolecular chemistry [32].

Considering the abovementioned facts, in the present study two aromatic *N*-heterocyclic ligands, phthalazine and quinazoline, reacted with different silver(I) salts. From these reactions, five new silver(I) complexes, three dinuclear **(1-3)** and two polynuclear **(4-5)**, were crystallized and structurally characterized. All these complexes were assessed for their in vitro antimicrobial and antiproliferative activities against normal human cell line to properly address their therapeutic potential. The DNA interaction properties of these complexes were also assessed experimentally and in silico.

2. Experimental section

2.1. Materials

Distilled water was demineralized and purified to a resistance of greater than 10 MΩ/cm. The starting silver(I) salts ($AgNO_3$, $AgCF_3SO_3$, $AgClO_4{\cdot}xH_2O$ and $AgBF_4$), ethanol, methanol, acetonitrile and dimethyl sulfoxide were purchased from Sigma-Aldrich. Phthalazine (phtz) and quinazoline (qz) were obtained from ABCR. All reactants were of analytical reagent grade and used without further purification.

*2.2. Synthesis of silver(I) complexes **1-5***

Silver(I) complexes with phthalazine and quinazoline, $\{[Ag(NO_3\text{-}O)(phtz\text{-}N)]_2(\mu\text{-}phtz\text{-}N,N')_2\}$ (**1**), $\{[Ag(CF_3SO_3\text{-}O)(phtz\text{-}N)]_2(\mu\text{-}phtz\text{-}N,N')_2\}$ (**2**), $\{[Ag(ClO_4\text{-}O)(phtz\text{-}N)]_2(\mu\text{-}phtz\text{-}N,N')_2\}$ (**3**), $\{[Ag(CF_3SO_3\text{-}O)(qz\text{-}N)]_2\}_n$ (**4**) and $\{[Ag(qz\text{-}N)][BF_4]\}_n$ (**5**), were synthesized according to the modified procedure for the preparation of silver(I) complexes with 2,3-diphenylquinoxaline [33].

The solution of 1.0 mmol of the corresponding silver(I) salt (169.9 mg of $AgNO_3$ for **1**, 256.9 mg of $AgCF_3SO_3$ for **2** and **4**, 207.3 mg of $AgClO_4{\cdot}xH_2O$ for **3** and 194.7 mg of $AgBF_4$ for **5**) in 5.0 mL of ethanol (**1** and **5**) or 5.0 mL of methanol (**2-4**) was added

slowly under stirring to the solution containing an equimolar amount (130.2 mg) of phthalazine (**1**-**3**) and quinazoline (**4** and **5**) in 20.0 mL of warm ethanol (**1** and **5**) or 20.0 mL of methanol (**2**-**4**). The reaction mixture was stirred in the dark at room temperature for 3 h. The solid product of complexes **1**, **3** and **5** precipitated during this time was filtered off and dissolved in 20.0 mL of acetonitrile. These complexes were crystallized after acetonitrile solutions were left to stand in the refrigerator for four days. The colorless crystals of these three complexes suitable for single-crystal X-ray crystallography were filtered off and dried in the dark at ambient temperature. However, complexes **2** and **4** were crystallized from mother methanol solution after its cooling in the refrigerator for several days. Yield (calculated on the basis of the *N*-heterocyclic ligand): 114.0 mg (53%) for **1**, 162.9 mg (63%) for **2**, 133.3 mg (57%) for **3**, 162.6 mg (42%) for **4** and 136.4 mg (42%) for **5**.

Anal. Calcd. for **1** = $C_{32}H_{24}Ag_2N_{10}O_6$ (M_r = 860.36): C, 44.67; H, 2.81; N, 16.28. Found: C, 44.45; H, 2.92; N, 16.13%. ^{1}H NMR (400 MHz, CD_3CN): δ = 8.02-8.06 (*m*, 8H, phtz), 8.10-8.14 (*m*, 8H, phtz), 9.59 ppm (*s*, 8H, phtz). ^{13}C NMR (101 MHz, CD_3CN): δ = 126.95 (C5 and C8), 126.99 (C4a and C8a), 133.55 (C6 and C7), 151.97 ppm (C1 and C4). IR (KBr, ν, cm^{-1}): 3035 (ν(Car–H)), 1618 and 1488 (ν(Car=Car)), 1568 (ν(Car=N)), 1440 (ν(N=N)), 1377 and 1362 (ν(NO_3)), 1301 (ν(Car–N)), 650 (γ(Car–H)). UV-vis (DMSO, λ_{max}, nm): 288.0 (ε = $2.9 \cdot 10^3$ $M^{-1}cm^{-1}$).

Anal. Calcd. for **2** = $C_{34}H_{24}Ag_2F_6N_8O_6S_2$ (M_r = 1034.47): C, 39.48; H, 2.34; N, 10.83. Found: C, 39.28; H, 2.51; N, 10.96%. ^{1}H NMR (400 MHz, CD_3CN): δ = 8.05-8.08 (*m*, 8H, phtz), 8.12-8.16 (*m*, 8H, phtz), 9.60 ppm (*s*, 8H, phtz). ^{13}C NMR (101 MHz, CD_3CN): δ = 127.07 (CF_3SO_3, C5 and C8), 127.10 (C4a and C8a), 133.86 (C6 and C7), 152.42 ppm (C1 and C4). IR (KBr, ν, cm^{-1}): 3041 (ν(Car–H)),

1619 and 1489 (ν(Car=Car)), 1564 (ν(Car=N)), 1445 (ν(N=N)), 1381 (*ν*(Car–N)), 1274 ($\nu_{as}(SO_3)$), 1256 ($\nu_{as}(CF_3)$), 1150 ($\nu_s(CF_3)$), 1031 ($\nu_s(SO_3)$), 636 (γ(Car–H)). UV-vis (DMSO, λ_{max}, nm): 290.0 ($\varepsilon = 3.6 \cdot 10^3$ $M^{-1}cm^{-1}$).

Anal. Calcd. for **3** = $C_{32}H_{24}Ag_2Cl_2N_8O_8$ (M_r = 935.23): C, 41.10; H, 2.59; N, 11.98. Found: C, 40.89; H, 2.71; N, 12.06%. ^{1}H NMR (400 MHz, CD_3CN): δ = 8.05-8.11 (*m*, 8H, phtz), 8.14-8.19 (*m*, 8H, phtz), 9.60 ppm (*s*, 8H, phtz). ^{13}C NMR (101 MHz, CD_3CN): δ = 126.55 (C5 and C8), 126.59 (C4a and C8a), 133.42 (C6 and C7), 152.02 ppm (C1 and C4). IR (KBr, ν, cm^{-1}): 3040 (*ν*(Car–H)), 1618 and 1489 (ν(Car=Car)), 1578 (ν(Car=N)), 1444 (ν(N=N)), 1378 (*ν*(Car–N)), 1158 and 1090 ($\nu(ClO_4)$), 623 (γ(Car–H)). UV-vis (DMSO, λ_{max}, nm): 290.0 ($\varepsilon = 2.8 \cdot 10^3$ $M^{-1}cm^{-1}$).

Anal. Calcd. for **4** = $C_{18}H_{12}Ag_2F_6N_4O_6S_2$ (M_r = 774.18): C, 27.93; H, 1.56; N, 7.24. Found: C, 28.10; H, 1.75; N, 7.35%. ^{1}H NMR (400 MHz, CD_3CN): δ = 7.78-7.85 (*m*, 2H, qz), 8.05-8.11 (*m*, 4H, qz), 8.11-8.18 (*m*, 2H, qz), 9.30 (*s*, 2H, qz), 9.55 ppm (*s*, 2H, qz). ^{13}C NMR (101 MHz, CD_3CN): δ = 125.20 (C8a), 127.85 (CF_3SO_3, C6 and C8), 128.45 (C7), 134.99 (C5), 149.47 (C4a), 155.31 (C4), 161.15 ppm (C2). IR (KBr, ν, cm^{-1}): 3060 (*ν*(Car–H)), 1621 and 1494 (ν(Car=Car)), 1584 (ν(Car=N)), 1383 (*ν*(Car–N)), 1280 ($\nu_{as}(SO_3)$), 1234 ($\nu_{as}(CF_3)$), 1163 ($\nu_s(CF_3)$), 1030 ($\nu_s(SO_3)$), 639 (γ(Car–H)). UV-vis (DMSO, λ_{max}, nm): 306.0 ($\varepsilon = 3.1 \cdot 10^3$ $M^{-1}cm^{-1}$).

Anal. Calcd. for **5** = $C_8H_6AgBF_4N_2$ (M_r = 324.83): C, 29.58; H, 1.86; N, 8.62. Found: C, 30.05; H, 2.08; N, 8.50%. ^{1}H NMR (400 MHz, CD_3CN): δ = 7.78-7.86 (*m*, 1H, qz), 8.04-8.09 (*m*, 2H, qz), 8.11-8.18 (*m*, 1H, qz), 9.28 (*s*, 1H, qz), 9.54 ppm (*s*, 2H, qz). ^{13}C NMR (101 MHz, CD_3CN): δ = 125.23 (C8a), 127.87 (C6), 127.90 (C8), 128.45 (C7), 134.96 (C5), 149.55 (C4a), 155.34 (C4), 161.13 ppm (C2). IR (KBr, ν, cm^{-1}): 3065 (*ν*(Car–H)), 1618 and 1493 (ν(Car=Car)), 1587

(ν(Car=N)), 1384 (*ν*(Car–N)), 1083 ($\nu_{as}(BF_4)$), 793 ($\nu_s(BF_4)$), 638(m) (γ(Car–H)). UV-vis (DMSO, λ_{max}, nm): 306.0 ($\varepsilon = 1.6 \cdot 10^3$ $M^{-1}cm^{-1}$).

Caution: There was no incident with $AgClO_4 \cdot xH_2O$ and complex **3** but care should be taken in handling these compounds as perchlorates are potentially explosive.

2.3. Measurements

Elemental analyses for carbon, hydrogen and nitrogen were performed on a Vario EL instrument by the Microanalytical Laboratory, Department of Organic Chemistry, University of Heidelberg. NMR spectra were recorded at 25 °C in acetonitrile-d_3 on a Bruker Avance II 400 MHz spectrometer. Chemical shifts are reported in ppm (δ). 10 mg of each complex was dissolved in 0.7 mL of acetonitrile-d_3 and transferred into a 5 mm NMR tube. Infrared spectra were recorded as KBr pallets on a Perkin Elmer Spectrum 100 spectrometer over the range of 450 – 4000 cm^{-1}. The UV-vis spectra were recorded on a Cary 100 spectrophotometer (Varian, USA), after dissolving of the corresponding silver(I) complex in dimethyl sulfoxide (DMSO), as well as after 24 and 96 h incubation at 37 ^oC, over the wavelength range of 200 – 900 nm. The concentration of the silver(I) complexes was 0.25 mg/mL.

2.4. Air/light stability of silver(I) complexes and salts

Air/light stability of complexes **1**-5, and the starting silver(I) salts was studied by indirect light in air atmosphere at room temperature. Sterile cellulose discs were impregnated with the silver(I) complexes and salts (200 µg/disc, using 50 mg/mL DMSO

stock solution) and exposed to air and light. The stability was monitored visually within 96 h.

2.5. X-Ray crystal structure determinations

Crystal data and details of the structure determinations are listed in the supplementary material (Table S1). Full shells of intensity data were collected at low temperature (100 K) with a Bruker AXS Smart 1000 CCD diffractometer (Mo-K_α radiation, sealed tube, graphite monochromator). Data were corrected for air and detector absorption, Lorentz and polarization effects [34]; absorption by the crystal was treated with a semi empirical multiscan method [35-38]. The structures were solved by the charge flip procedure [39,40] and refined by full-matrix least squares methods based on F^2 against all unique reflections [41-43]. All non-hydrogen atoms were given anisotropic displacement parameters.

Hydrogen atoms were generally input at calculated positions and refined with a riding model. When justified by the quality of the data the positions of the hydrogen atoms were taken from difference Fourier syntheses and refined. When found necessary, disordered groups were subjected to suitable geometry and adp restraints. The nitrate group in complex **1** was found to be disordered around its pseudo threefold axis over two sites, resulting in a more strongly (refined population 0.89(1); d(Ag–O1a) = 2.576(4) Å) and a much more weakly Ag-O binding situation (refined population 0.11(1); d(Ag–O1a) = 3.19(4) Å). In complex **4,** the biggest difference Fourier peaks, 2.37 and 2.22 e/Å^3, are 1.1 Å from C1 and 1.0 Å from C9, respectively. In complex **5** the biggest difference Fourier peak, 2.75 e/ Å^3, is 0.8 Å from Ag and likely due to absorption. MERCURY computer graphics program [44] was used to prepare drawings.

2.6. Disc-diffusion assay and minimum inhibitory concentration (MIC) determination

Test organisms for the antibacterial assays were obtained from the National Collection of Type Cultures (NCTC) and the American Type Culture Collection (ATCC). They included two Gram positive strains (*Staphylococcus aureus* NCTC 6571 and *Enterococcus faecalis* ATCC 29212) and two Gram negative strains (*Escherichia coli* NCTC 9001 and *Pseudomonas aeruginosa* PAO1 NCTC 10332) as well as *Candida albicans* ATCC 10231. Two clinical isolates of *P. aeruginosa* MD-49 and MD-50 with high ability to form biofilms and resistance to metronidazole, clindamycin and amoxicillin were also included in the study.

Standard disc diffusion assay was done for the preliminary screen using 0.2 mg of test compounds per disc. Briefly, late stationary phase cells of test microorganisms were spread on nutrient agar plates and sterile cellulose discs (6 mm diameter) were applied to the surface (HiMedia Laboratories, Mumbai, India). Plates were incubated at 37 ^{o}C and zones of inhibition were measured. As a control, kanamycin solution (0.02 mg/disc) was also included in the antimicrobial disc diffusion assay.

MIC concentrations of **1-5**, precursor ligands and respective starting salts were determined according to standard broth micro dilution assays recommended by the National Committee for Clinical Laboratory Standards (M07-A8) for bacteria and Standards of European Committee on Antimicrobial Susceptibility Testing (EDef7.1.) [45]. Tested compounds were dissolved in DMSO. The highest concentration used was 500 μg/mL, *i.e.* $5.8 \cdot 10^{-4}$ (**1**), $4.8 \cdot 10^{-4}$ (**2**), $5.4 \cdot 10^{-4}$ (**3**), $6.5 \cdot 10^{-4}$ (**4**), $1.5 \cdot 10^{-3}$ (**5**), $2.9 \cdot 10^{-3}$ ($AgNO_3$), $2.6 \cdot 10^{-3}$ ($AgBF_4$), $2.4 \cdot 10^{-3}$ ($AgClO_4 \cdot xH_2O$) and $1.9 \cdot 10^{-3}$ M ($AgCF_3SO_3$). The inoculums were 10^5 colony forming units (cfu) per mL

for bacteria, and 10^4 cfu/mL for *Candida albicans*. The MIC value corresponds to the lowest concentration that inhibited the growth after 24 h at 37 °C. The $AgNO_3$ salt was considered as positive control, as it has been used clinically [18].

2.7. Viability analysis of silver(I)-treated P. aeruginosa PAO1

To examine the bactericidal effect of silver(I) complexes on free living cells, *P. aeruginosa* PAO1 was subcultured in fresh LB broth and incubated at 37 °C for 6 h with MIC of silver(I) complexes, whereas cells incubated with DMSO were taken as control. After 30 min, 3 and 6 h, an aliquot of culture (1.0 mL) was centrifuged at 10000 x g for 3 min. Cells were washed twice with sterile 0.9% NaCl and finally resuspended in 1 mL of sterile 0.9% (w/v) NaCl. To carry out the Live/Dead staining, 10^7 cfu/mL was stained with 5 µM SYTO9 green fluorescent dye and 45 µM propidium iodide (PI) red fluorescent dye of Live/Dead staining kit (LIVE/DEAD® BacLight™ Bacterial Viability Kit, Thermo Fisher Scientific, Waltham, MA, USA) in 500 µL of 0.9% NaCl. The samples were analyzed on a flow cytometer (CyFlow Space, Partec, GmbH, Münster, Germany) to discriminate between live and dead cells. Stained samples were also visualized using fluorescent microscopy at 100× magnification.

2.8. Inhibition of formation and disruption of P. aeruginosa biofilms

Biofilm quantification assays were performed in microtiter plate format using a crystal violet staining of adherent cells [46]. Overnight cultures of *P. aeruginosa* strains were subcultured at 37 °C in TSB medium (HiMedia Laboratories) with and without test compounds in a 96-well microtiter plates. After 24 h growth free (detached) cells were removed, wells were washed with PBS and biofilms fixed

with 100 µL of 99% (v/v) methanol followed by staining with 0.4% (v/v) crystal violet. After washing, crystal violet was solubilised with 150 µL of glacial acetic acid (33%, v/v) and absorbance was measured at 540 nm. The biofilm formation assay was performed in six wells and repeated twice.

Biofilm disruption assay was performed in 24-well microtiter plate as previously described [47]. *P. aeruginosa* cultures were grown overnight in M9 medium at 37 °C with shaking at 180 rpm and subcultured in 24-well microtiter plate (1% v/v inoculums in 1 mL M9 medium supplemented with 20 mM glucose) and further incubated at 37 °C with 180 rpm shaking. Test compounds were added at concentration of 10 µg/mL *i.e.* 11.6 (**1**), 9.7 (**2**), 10.7 (**3**), 12.9 (**4**), 30.8 (**5**), 58.9 ($AgNO_3$), 51.4 ($AgBF_4$), 48.2 ($AgClO_4 \cdot xH_2O$) and 38.9 µM ($AgCF_3SO_3$) after 6 h of growth. After 1 h free (detached) cells were removed, wells washed with PBS and adherent cells were stained with crystal violet.

2.9. Live/Dead staining of the bacterial biofilms

To study the effect of silver(I) complexes on *P. aeruginosa* PAO1 biofilms, overnight bacterial culture grown in LB medium was diluted to optical density OD600 of 0.05 in M9 medium and the biofilms were grown on glass cover slips in the presence of 10 µg/mL, *i.e.* 11.6 (**1**), 9.7 (**2**), 10.7 (**3**), 12.9 (**4**), 30.8 (**5**), 58.9 ($AgNO_3$), 51.4 ($AgBF_4$), 48.2 ($AgClO_4 \cdot xH_2O$) and 38.9 µM ($AgCF_3SO_3$) of the silver(I) compounds or DMSO. After 24 h growth at 37 °C, biofilms were washed with 0.9% (w/v) NaCl and stained with 2.5 µM SYTO9 green fluorescent dye and 2.5 µM propidium iodide (PI) red fluorescent dye of Live/Dead staining kit (LIVE/DEAD® BacLight™ Bacterial Viability Kit, Thermo Fisher Scientific, Waltham, MA, USA). Biofilms and cells were observed under a fluorescence

microscope (Olympus BX51, Applied Imaging Corp., San Jose, USA) at 100 × magnification.

2.10. Assessment of P. aeruginosa motility

Twiching motility was evaluated as previously described [8]. *Pseudomonas* culture was stabbed with a toothpick into LB plates supplemented with 1% agar containing various concentrations of silver(I) complexes, salts or DMSO and incubated overnight at 37 °C for 20 h and incubation continued for additional 72 h at 25 °C. Bacterial migration along the plastic surface was detected by crystal violet (2%, (v/v)) staining after removing the agar from the plate. Twitching motility was determined by measuring the diameter of the stained areas.

Swimming motility was measured according to previously described protocol [48]. Diluted bacteria were point-inoculated onto M8 plates (5 g Na_2HPO_4, 3 g KH_2PO_4, 0.5 g NaCl, 0.2% glucose, 0.5% casaminoacids and 1 mM $MgSO_4$) containing 0.3% (w/v) agar supplemented with 0.5 MIC of silver(I) complexes or salts. The plates were incubated for 18 h at 37 °C. The distance of colony migration around the inoculation site was measured and compared to *P. aeruginosa* inoculated onto plates with DMSO. A swarming assay was performed on M8 plates containing 0.8% agar supplemented with 0.5 MIC of silver(I) complexes or salts. Plates were inoculated with 2.5 μL of the diluted *Pseudomonas* cultures and the phenotype was observed after 16 h incubation at 37 °C [49].

2.11. Antiproliferative activity by MTT assay

Cell viability was tested by MTT (3-(4,5-dimethylthiazol-2-yl)-2,5-diphenyltetrazolium bromide) assay [50]. Assay was carried out using human lung

fibroblastic cell line (MRC5) after 48 h of cell incubation in the media containing test compounds at concentrations ranging from 0.1 (0.1 (**1**-**4**), 0.3 (**5**), 0.6 ($AgNO_3$), 0.5 ($AgBF_4$ and $AgClO_4 \cdot xH_2O$) and 0.4 μM ($AgCF_3SO_3$)) to 100 μg/mL (116.2 (**1**), 96.7 (**2**), 106.9 (**3**), 129.2 (**4**), 307.9 (**5**), 588.7 ($AgNO_3$), 513.7 ($AgBF_4$), 482.3 ($AgClO_4 \cdot xH_2O$) and 389.2 μM ($AgCF_3SO_3$). MRC5 cell line was maintained in RPMI-1640 medium supplemented with 100 μg/mL streptomycin, 100 U/mL penicillin and 10% (v/v) fetal bovine serum (FBS) (all from Sigma, Munich, Germany), as a monolayer (1 x 10^4 cells per well) and grown in humidified atmosphere of 95% air and 5% CO_2 at 37 °C.

The extent of MTT reduction was measured spectrophotometrically at 540 nm using Tecan Infinite 200 Pro multiplate reader (Tecan Group Ltd., Männedorf, Switzerland) and the cell survival was expressed as percentage of the control (untreated cells). The percentage viability values were plotted against the log of concentration and a sigmoidal dose response curve was calculated by non-linear regression analysis using Graphpad Prism software version 5.0 for Windows (Graphpad Software, CA, USA). Cytotoxicity is expressed as the concentration of the compound inhibiting growth by 50% (IC_{50}).

2.12. In vitro DNA binding by gel electrophoresis assay

Genomic DNA (gDNA) from *P. aeruginosa* PAO1 was purified with a DNeasy tissue kit (Qiagen, Hilden, Germany). The quality and the concentration of DNA were estimated by measuring UV absorbance with a NanoVue Plus spectrophotometer (GE Healthcare, Freiburg, Germany). The ability of **1**-**5** and respective silver(I) salts to bind gDNA from *P. aeruginosa* PAO1 was examined by using agarose gel electrophoresis [51,52]. For the gel electrophoresis experiments,

gDNA (500 ng) was treated with 25 μg/mL (29.1 (**1**), 24.2 (**2**), 26.7 (**3**), 32.3 (**4**), 77.0 (**5**), 147.2 ($AgNO_3$), 128.4 ($AgBF_4$), 120.6 ($AgClO_4{\cdot}xH_2O$) and 97.3 μM ($AgCF_3SO_3$) of the salts and complexes in phosphate buffer (pH 7.4), and the contents were incubated for 12 h at 37 °C, then subjected to gel electrophoresis on 0.8% (w/v) agarose gel containing 0.1 μg/mL of ethidium bromide in TAE buffer (40 mM Tris acetate/1 mM EDTA, pH 7.4) at 60 V for 2 h. Gels were visualized and analyzed using the Gel Doc EZ system (Bio-Rad, Life Sciences, Hercules, USA), equipped with the Image Lab™ Software.

2.13. In silico studies of the interaction of DNA with the metal complexes

The interaction of DNA with the metal complexes was studied by molecular docking. The silver(I) complexes were geometry optimized using semi-empirical quantum chemistry (PM6) because of its excellent compromise between computational time and description of the electronic correlation [53-55]. All geometry optimization calculations were performed with the Gaussian 09 software package [56]. The structure of the B-DNA dodecamer (CGCGAATTCGCG)2 (PDB code 1BNA) [57] was used as a model to study the interaction between the silver(I) complex and DNA [58,59]. Crystallographic water molecules were removed from the DNA fragment. The DNA···silver(I) complex interaction was studied using the Patch dock web server [60]. The resulting poses were used for further refinement with FireDock [61]. The visualization of lowest energy poses was done using CHIMERA (http://www.cgl.ucsf.edu/chimera/) molecular graphics program.

3. Results and discussion

*3.1. Synthesis and structural characterization of the silver(I) complexes **1-5***

Two aromatic *N*-heterocycles, phthalazine (phtz) and quinazoline (qz), were used as ligands for silver(I) complexes, using different AgX salts (X = NO_3^-, $CF_3SO_3^-$, ClO_4^- and BF_4^-) (Scheme 1). Both *N*-heterocycles contain two nitrogen atoms at different positions in one ring, 2,3 for phtz and 1,3 for qz. These isomers have different steric and electronic properties and therefore are likely to provide different structural motifs. All reactions were performed by mixing equimolar amounts of the reactants at room temperature in ethanol or methanol. Despite the use of different silver(I) salts, phtz reacted with all to form similar dinuclear species of the general formula {[Ag(X-*O*)(phtz-*N*)]$_2$(μ-phtz-*N,N'*)$_2$}, X = NO_3^- (**1**), $CF_3SO_3^-$ (**2**) and ClO_4^- (**3**) (Scheme 1a). In contrast, the reactions of qz with an equimolar amount of $AgCF_3SO_3$ and $AgBF_4$, led to the formation of polynuclear silver(I) complexes, {[Ag(CF_3SO_3-*O*)(qz-*N*)]$_2$}$_n$ (**4**) and {[Ag(qz-*N*)][BF_4]}$_n$ (**5**) (Scheme 1b). The stoichiometries of **1-5** were confirmed by elemental microanalysis, and the structures emerge from NMR (^{1}H and ^{13}C) and IR spectroscopy as well as single-crystal X-ray diffraction analysis.

Scheme 1

3.1.1. Description of the single crystal structures

Suitable single crystals of **1** and **3** were grown from acetonitrile, and those of **2** were obtained by slow evaporation from methanol. The molecular structures of **1-3** are very similar, composed of a six-membered dimetallic ring, which is formed by the two silver(I) centers and the corresponding nitrogen atoms of two phthalazines.

These two phtalazines act as bridging ligands between two silver(I) ions, while the remaining two are monodentately coordinated to silver(I). The corresponding anion X (X = NO_3^- in **1**, $CF_3SO_3^-$ in **2** and ClO_4^- in **3**) is weakly coordinated through one oxygen atom to the silver(I) centers. ORTEP-type drawings of **1-3** are shown in Fig. 1, accompanied by the crystal packing in Fig. S1. There are two independent half-molecules of **2** in the asymmetric unit, with virtually identical $Ag_2(phtz)_2$ cores and slightly different orientations of the triflate anions.

Fig. 1

Complexes **1**-**3** have four-coordinate, distorted tetrahedral silver(I) ions. Houser et al. [62] proposed a parameter (τ_4) as a simple metric for quantitatively evaluating the geometry of four-coordinate metal complexes, $\tau_4 = [360^o - (\beta + \alpha)]/141^o$, where β and α are the largest angles involving the metal center. Perfectly square-planar and tetrahedral geometries result in τ_4 values of 0 and 1, respectively [62]. For the silver(I) complexes **1-3**, τ_4 = 0.80 (**1**), 0.80/0.77(**2**) and 0.77 (**3**), that is, the structures are distorted tetrahedral. The Ag–N bond distances adopt values of 2.256(1) – 2.306(1) Å (**1**), 2.256 (2) – 2.346(2) Å (**2**) and 2.251(2) – 2.317(2) Å (**3**) (Table 1) and compare well with those found in the other pseudo tetrahedral silver(I) complexes [26,63,64]. On the other hand, the Ag–O bond distances of 2.576(4) (**1**), 2.533(2)/2.560(2) (**2**) and 2.642(2) Å (**3**) (Table 1), are much longer than usual covalent silver(I)–oxygen bonds of about 2.3 Å [26]. This indicates that nitrate, trifluoromethanesulfonate and perchlorate in **1**, **2** and **3** are only weakly bound to the silver(I) ions. A very week Ag···Ag intramolecular interaction is observed only in **1**, at an Ag···Ag distance of 3.434(1) Å, which is longer than the commonly

reported Ag···Ag bond range of 2.853 – 3.290 Å [65], and only slightly shorter than the sum of van der Waals radii (3.44 Å) [66]. In silver metal, the Ag···Ag distance is 2.88 Å [67].

Table 1

Contrary to the dinuclear phtz-silver(I) complexes **1-3**, the previously characterized $\{[Ag(\mu\text{-}CH_3COO\text{-}O,O')(\mu\text{-phtz-}N,N')(H_2O)_2]_2\}_n$ complex has polymeric structure [68]. This structure comprises stacks of phtz-bridged silver(I) dimeric $Ag_2(phtz)_2$ subunits; these subunits are further connected by the acetates which bridge these stacks to form a polymer. The acetate anions form an asymmetric four-membered chelate rings with the silver(I) ion, resulting in its distorted square pyramidal geometry. Furthermore, tetranuclear $[Ag_4(\mu\text{-phtz-}N,N')_7](NTf_2)_4$ complex was obtained in the reaction of silver(I) triflimide ($AgNTf_2$) with phtz [69]. In the cation of this complex, two pseudo-tetrahedral silver(I) centers are bridged by three phtz ligands, while the other two have trigonal geometry and are briged by two phtz units. The remaining two phtz ligands form the bridging units between one pseudo-tetrahedral and one trigonal silver(I) ions. On the other hand, the reaction of $AgNTf_2$ with phtz in the presence of 2,2':6',2''-terpyridine (terpy), led to the formation of the dinuclear $[Ag_2(\mu\text{-phtz-}N,N')(terpy)_2](NTf_2)_2{\cdot}2CH_3CN$ complex [69].

Both **4** and **5** have coordinated quinazoline ligand and are polymeric species. Their asymmetric units are displayed in Fig. 2, while the crystal packing is given in Fig. S2. The asymmetric unit of the coordination polymer **4**, formed in the reaction of quinazoline with $AgCF_3SO_3$, comprises two independent silver(I) centers, Ag1

and Ag2, two quinazoline heterocycles and two $CF_3SO_3^-$ anions (Fig. 2). The Ag1–N and Ag2–N bonds distances in **4** (Table 2) compare well with those found in the silver(I) complexes **1-3**, as well as other pseudo tetrahedral silver(I) complexes [26,63,64]. Complex **5** is a 1D coordination polymer with a zigzag conformation. The two independent silver(I) centers in this complex, Ag1 and Ag2, are coordinated by two nitrogen atoms from two different quinazoline ligands, *i.e.* quinazoline acts as a bridging ligand between two silver(I) ions (Fig. 2). The Ag1–N bond lengths are 2.147(4) and 2.142(4) Å, while the lengths of the corresponding Ag2–N bonds are 2.126(4) and 2.141(4) Å (Table 2). Each silver(I) ion adopts a slightly distorted linear geometry, with N3—Ag1—N1 and N2—Ag2—N4 angles of 177.0(2) and 172.7(2) °, respectively (Table 2). In **4** and **5**, there are no Ag···Ag interactions, and the distances between two silver(I) ions are much larger than the sum of the van der Waals radii (3.44 Å) [66].

Table 2 and Fig. 2

3.1.2. IR spectroscopic characterization

The IR data of **1-5**, listed in the Experimental Section, are consistent with the structures determined by X-ray crystallography. Except for the peaks that are relevant for the coordinated phtz and qz ligands, the IR spectra of the complexes also show the typical peaks of the corresponding anion. Moreover, a detailed analysis of this part of the IR spectra of **1-5**, may give an insight in the nature of coordination of the anions. In the spectrum of **1**, the strong bands at 1377 and 1362 cm^{-1} and two very week in the overtone region (1700 – 1800 cm^{-1}) can be ascribed to the nitrate group (asymmetric and symmetric stretching modes and combination

of symmetric stretching and in-plane bending, respectively) [70]. The presence of two bands in the overtone region is an indication of a monodentate coordination of nitrate (bidentate nitrate groups also gives rise to two frequencies in the overtone region, but with wider separation) [71]. The IR spectra of **2** and **4** show a number of strong absorptions in the 1000 – 1300 cm^{-1} region. These bands at 1274 and 1031 cm^{-1} (**2**), and at 1280 and 1030 cm^{-1} (**4**) are ascribed to the asymmetric and symmetric stretching modes of $–SO_3$ group in $CF_3SO_3^-$ anion [72]. The remaining two bonds at 1256 and 1150 cm^{-1} (**2**), and at 1234 and 1163 cm^{-1} (**4**) are due to the asymmetric and symmetric stretching modes of $–CF_3$ group in $CF_3SO_3^-$ anion. In the spectrum of **3**, the presence of two strong absorption bands at 1158 and 1090 cm^{-1} indicates a monodentate coordination mode of ClO_4^- [73]. Also, non coordination of BF_4^- in **5** can be confirmed by the presence of the strong broad band at 1083 cm^{-1} and a medium one at 793 cm^{-1} in its IR spectrum [74].

*3.2. Stability of complexes **1-5***

3.2.1. Solution stability

An essential prerequisite for the biological evaluation of metal complexes as antimicrobial agents is their stability in solution [75]. In order to investigate the stability of **1-5**, they were dissolved in DMSO, and their UV-vis spectra were recorded after dissolution, as well as after 24 and 96 h of incubation at 37 ^oC. The wavelengths of maximum absorption (λ_{max}, nm) and molar extinction coefficients (ε, $M^{-1}cm^{-1}$) for the investigated complexes **1-5,** determined directly after dissolution in DMSO, are listed in the Experimental Section. In all these complexes, the corresponding absorbance peaks are due to $\pi \rightarrow \pi^*$ transitions in the aromatic *N*-heterocycles [76] but they show slight red shifts compared to those in the free

ligands (λ_{max} = 288.0 for phtz and λ_{max} = 304.0 nm for qz). Moreover, the shape of spectra and values of λ_{max} are very similar for **1-3** with phtz and **4-5** with qz, indicating the same coordination mode of the corresponding *N*-heterocycle to the silver(I) ion. From the UV-vis spectra recorded during time it can be concluded that all investigated complexes are stable in DMSO for up to 96 h at 37 ^{o}C and only minor changes in the intensity of the absorption maxima were observed under these circumstances. As an illustration, the UV-vis spectra of **3** and **5** are presented in Fig. S3 as a function of time.

3.2.2. Air/light stability

In order to investigate the air/light stability of the silver(I) complexes **1-5** and the corresponding salts, sterile cellulose discs impregnated with these compounds were exposed to air and light for 96 h (Fig. S4). As can be seen from Fig. S4, all investigated silver(I) compounds started to be a little beige after 24 h, and after 96 h all were slightly darker, indicating that slow light decomposition processes occurred during this time. Among the investigated silver(I) compounds, complex **1** qualitatively showed slightly higher air/light stability.

*3.3. Antimicrobial activity and antiproliferative effect of **1-5***

The silver(I) complexes **1-5**, along with the corresponding silver(I) salts, exhibited potent antimicrobial activity, while there was no significant antimicrobial activity with the ligands phtz and qz (Table 3). Due to its clinical relevance, $AgNO_3$ was used as a control. We also present a comparative antimicrobial assessment of other silver(I) salts, *i.e.* $AgCF_3SO_3$, $AgBF_4$ and $AgClO_4 \cdot xH_2O$. Importantly, **1-5** were active against all tested strains that included Gram-negative *P. aeruginosa*

PAO1 and *E. coli*, Gram-positive *S. aureus* and *E. faecalis*, as well as fungus *C. albicans*, from moderate to very good and with broad spectrum. The selection of microorganisms was due to their usual coexistence in persistent infections. Chronic wounds are frequently colonized by an assembly of bacteria, which include *P. aeruginosa* and *S. aureus*, obligate anaerobes, as well as filamentous fungi and yeasts, such as *Candida* spp. [77].

Table 3

With **1-5**, the best activity was detected against *P. aeruginosa* PAO1 with MIC values between 2.9 and 29 μM, which was comparable to or up to 6-fold lower than MIC of $AgNO_3$. Importantly, marked activity against multi-antibiotic resistant clinical isolates of *P. aeruginosa* MD-49 and MD-50 was also observed (Table 3). These pathogenic strains required smaller amounts of **4** and **5** but 2 to 7.5-fold larger amounts of **1-3** in comparison to the amounts required for *P. aeruginosa* PAO1, for an efficient inhibition (Table 3). Larger amounts of $AgNO_3$ were also needed to efficiently kill clinical *Pseudomonas* isolates. Obtained results are especially important when compared to cytotoxicity of these compounds to normal human fibroblasts which was lower except for **3**, having in mind that cytotoxicity of $AgNO_3$ was higher in comparison to all MIC values (Table 4). Phtz-containing complex **1** stood out with 7.2-fold lower MIC against *P. aeruginosa* PAO1 in comparison to IC_{50}, suggesting wider therapeutic potential of this complex.

The activity of the complexes was excellent in the case of the Gram-positive *S. aureus* with the best MIC values of 8.3 and 9.1 μM for **3** and **1**, respectively. These were around 2-fold better in comparison to MICs of $AgNO_3$ against this

bacterium (Table 3). Moderate activity was determined against the Gram-positive opportunistic pathogen *E. faecalis* and yeast fungus *C. albicans*, with MIC concentrations between 16.7 and 48 μM, and 48.3 and 77 μM, respectively, compared to MICs of $AgNO_3$ against these microorganisms of 58.9 and 294.3 μM (Table 3).

In general, silver(I) salts exhibited comparable or lower MIC values in comparison to **1-5** values against the tested microorganisms. However, the cytotoxicity of silver(I) salts was <10 μM and therapeutic index consistently negative (Table 4). The most cytotoxic salts were $AgClO_4 \cdot xH_2O$ and $AgBF_4$, which had a 4-fold and 3.5-fold higher cytotoxicity in comparison to **5** and **1**, respectively (Table 4). Note that the molar ratio of silver(I) ions in salts is considerably greater than in complexes: with $AgNO_3$, it is 1.9 to 3-fold greater than in **5** and **2**, respectively. MIC concentrations reported for silver ions against different bacteria range from 60-180 μM (10-30 μg/mL) [21,78], while MIC against *P. aeruginosa* was determined to be 24 μM [79], which is similar to our study. Based on different and in some cases lower MIC values of the complexes in comparison to silver(I) salts, we concluded that the antimicrobial effect of the complexes is not solely due to the silver(I) ions and that it is rather multifactorial. This was not the case with silver(I) complexes of 2-hydroxymethyl-*N*-alkylimidazole, where the antibacterial activity was essentially the same as that of $AgNO_3$ and therefore assumed to be due to silver(I) ions [80].

Table 4

Among the complexes, **3** exhibited the best antibacterial properties across the tested range of microorganisms, but this was also coupled with similar or higher levels of undesired cytotoxicity (Tables 3 and 4). The complex **3** contains phtz and ClO_4^- (Fig. 1), which both may relate to its specific activity. However, the best activity profile was exhibited by **1**, having coordinated nitrate and phtz (Fig. 1), with low MIC values against bacteria, especially *P. aeruginosa* and low cytotoxicity of 20.9 μM (Tables 3 and 4). Both, phtz and qz were found to be moderately cytotoxic with IC_{50} values in the 700-800 μM range (Table 4), and to have no significant antimicrobial activity. The time-kill assay and visualization, performed with the *P. aeruginosa* PAO1 strain, indicated that none of the complexes nor salts at the relatively high concentration of 10 μg/mL had toxic effects on this strain after 30 min (Fig. S5). After a 3 h incubation, apart from **1**, all other silver(I) compounds induced bacterial death, demonstrated by the appearance of 28-32% propidium iodide (PI) positive bacteria, as determined by flow cytometry (Fig. S5). In 6 and 12 h, all bacteria were PI positive (dead). After 3 h incubation, complex **1** induced 42.5% bacterial death, suggesting a different mode of action, presumably involving the bacterial membrane as the primary target (Fig. S5).

From our results it is not clear whether the silver(I) complexes were more active against Gram-positive or Gram-negative bacteria; however, they exhibited obviously low activity against fungus *C. albicans*. Silver(I) complexes of 2-hydroxymethyl-*N*-alkylimidazole and of the metronidazole drug showed a similar behavior [80,81]. Moreover, silver(I) complex with (*Z*)-3-(1H-imidazol-1-yl)-2-phenylpropenenitrile had a lower antifungal activity than the prescription drug, ketoconazole, and $AgClO_4$ [82]. There is no general rule in terms of the performance of silver(I) complexes against Gram-positive in comparison to Gram-

negative bacteria. The difference in the antimicrobial activity is usually associated with structural differences in the cell membrane of the microorganisms. Gram-positive bacteria have the membrane mainly composed of peptidoglycans, Gram-negative bacteria have an additional outer membrane composed of lipopolysaccharides, while cell wall of *Candida* is mainly composed of glucan, chitin and mannoproteins. We observed that the best activity of silver(I) complexes was achieved against the important opportunistic pathogen *P. aeruginosa* PAO1, with MIC values better than those reported so far [79,83]. More importantly, **1**-**5** exhibited good activities against multi-antibiotics resistant *P. aeruginosa* clinical isolates, which prompted further experiments with these strains.

Recently, silver(I) complexes with a number of different ligands have been studied for their antitumor activities, some of them showing antiproliferative activities higher than cisplatin [84,85]. Our study indicated that the cytotoxic activity of the silver(I) complexes discussed here was moderate and lower than that of $AgNO_3$ and therefore prompted further studies of these compounds as possible antimicrobial agents. On the other hand, di- and polynuclear silver(I) saccharinate complexes with tertiary monophosphines showed significant activity towards different bacterial strains (MIC = 14.5 – 114.6 μM), however they were also highly cytotoxic toward the human fibroblastic cell line WI-38 (IC_{50} = 0.74 – 1.41 μM) [52]. Similarly, silver(I) complexes with the ligands based on oligomers of polyethylene glycol, functionalized at both ends with either nicotinic or isonicotinic acid manifested a strong effect toward *Staphylococcus epidermidis* 1457 with the MIC values in the range 3.9 – 7.8 μg/mL (6.9 – 22.4 mmol Ag^+/mL) and high citotoxicity toward L-929 fibroblast murine cell line (IC_{50} = 16.53 – 28.65 mmol Ag^+/mL) [86].

*3.3.1. Effect of **1-5** on P. aeruginosa motility*

The initiation of biofilm formation by *P. aeruginosa* depends on two cell-associated structures, the flagellum and type IV pili [87,88]. The flagellum is responsible for swimming motility while the type IV pili are responsible for twitching motility. Both types of motility are important in the initial stages of biofilm formation by *P. aeruginosa* [87,88]. We therefore examined if complexes **1-5** and the corresponding silver(I) salts influenced motility in *P. aeruginosa* PAO1 and two *P. aeruginosa* clinical isolates (Table 5). On motility assessment plates, the motile strains PAO1, MD-49 and MD-50 were used as the control for motility (100%), while the Petri dishes with the same strain containing 0.5 MIC of the test compound were compared to that of the control with no treatment (Fig. S6).

Table 5

Based on the observation that MD-50 exhibited an 1.8- and 3-fold higher ability to form biofilms and produce piocyanin (indicator for a higher virulence of this isolate, results not shown), in comparison to *P. aeruginosa* PAO1, and that MD-49 produced piocyanin to a comparable level and had the 1.6-fold higher ability to form biofilms, it was not surprising that they exhibit different patterns of motility and a different response to the silver(I) compounds.

P. aeruginosa isolates produced swimming zones to 100% with a size of 14.0-25.5 mm (Fig. S6a). Swimming motility of PAO1 was affected more than of MD-49, while that of the MD-50 isolate was roughly unaffected (Table 5). The swimming zone diameter of the *P. aeruginosa* isolate MD-49 decreased between 13 and 36% in the presence of silver(I) salts and complex **2**, respectively. After 3 days

of incubation at ambient temperature, a colony expansion occurred very rapidly due to twitching motility (Fig. S6b). Twitching motility was affected in all three isolates, with silver(I) salts exhibiting higher efficiency on average than the complexes (Table 5). Bacteria that were grown with silver(I) compounds were incapable of producing twitching zones and had almost round, smooth, regular colony edges (Fig. S6b). Swarming motility was affected the least, with only the *P. aeruginosa* isolate MD-49 showing substantially decreased swarming in the presence of complex **5** and $AgClO_4 \cdot xH_2O$ (Table 5; Fig. S6c). We have demonstrated that the silver(I) complexes **1**-**5** had the potential to inhibit motility of *P. aeruginosa* isolates, which is one of the multicellular virulence markers in this strain and described to be associated with the biofilm formation in this strain [11].

*3.3.2. Activity of **1-5** against P. aeruginosa biofilms*

P. aeruginosa is a highly successful opportunistic pathogen that displays intrinsic multidrug resistance and has a tremendous capacity to acquire further resistance mechanisms [9]. During chronic infection, the bacterium usually grows as a biofilm, which is a protective mode of growth and allows resistance to existing antibiotics, and therefore is the origin of the majority of hospital-acquired infections [89]. Biofilms are known to be more tolerant to antimicrobial agents than rapidly growing cells in liquid cultures [10]. Based on a crystal violet microtiter assay, silver(I) complexes and salts inhibited biofilm formation of *P. aeruginosa* strains, when supplied in a concentration of 4 μg/mL to the medium that promoted biofilm formation (Fig. 3a).

Fig. 3

After 24 h of cultivation in the presence of the compounds, formation of *P. aeruginosa* PAO1 biofilms was decreased by 50% and 27% with **1** and **5**, respectively, in comparison to the untreated control. $AgCF_3SO_3$ inhibited *P. aeruginosa* PAO1 biofilm formation up to 45%, while the other silver(I) compounds are less effective, with inhibition rates between 23 and 31%. Interestingly, the complexes were more efficient (1.4-fold in average) in the inhibition of biofilm formation by the multidrug resistant clinical isolate MD-49 but for MD-50, the presence of salts stimulated biofilm formation, while the complexes reduced it between 33% and 16% (Fig. 3a).

Among the complexes, **1** and **2** had excellent and comparable activity across the range of *P. aeruginosa* strains, while **5** exhibited the highest activity against the multiantibiotic resistant clinical isolates MD-49 and MD-50 biofilm formation, with inhibition rates of 27% and 33%, respectively. We concluded that our silver(I) complexes had a better activity in the prevention of biofilm formation of pathogenic *P. aeruginosa* strains than $AgNO_3$ and other silver(I) salts.

Biofilms are characteristic for chronic wounds [90]. It was shown that *P. aeruginosa* colonizes on average more than 54% chronic wounds and that these wounds are significantly larger and more difficult to treat than wounds that do not contain *P. aeruginosa* [7]. To address the important effect of silver(I) compounds on preformed biofilms of *P. aeruginosa* PAO1 and clinical isolates, bacteria were cultured for 6 h in a biofilm formation promoting medium to allow adherence, and the biofilm disruption was induced for 1 h by addition of 10 μg/mL of all silver(I) compounds (Fig. 3b). Based on crystal violet staining, all complexes caused a 40-50% disruption of *P. aeruginosa* PAO1 biofilms. This was confirmed by live-dead staining and fluorescent microscopy (Fig. 3c). In the same assay, silver(I) salts

showed a better activity than the complexes, disrupting biofilms of *P. aeruginosa* PAO1 on average by 80% (Fig. 3b). Complexes **3** and **4** showed a higher efficiency (57% and 59% disruption, respectively) when a preformed biofilm of the clinical isolate MD-49 was treated. Biofilms of the clinical isolate MD-49 were resistant to **1**, indicating strain specificity. Interestingly, silver(I) salts induced between 30% and 70% cell detachment in the clinical isolate MD-49. Under the conditions of the experiments, biofilms formed by the clinical isolate MD-50 were resistant to all silver(I) complexes and the most of corresponding silver(I) salt treatments, as only $AgNO_3$ caused up to 20% biofilm disruption. In conclusion, the silver(I) complexes with phthalazine and quinazoline are effective in the disruption of preformed *P. aeruginosa* biofilms in the concentration range of 10μg/mL, and this activity is strain dependent. Previous studies indicate that silver(I) salts in concentrations much larger than MIC values for the free cells growing in liquid cultures can eliminate fully developed *P. aeruginosa* PAO1 biofilms, and it was also shown that *P. aeruginosa* PAO1 is not able to form biofilms on silver-coated urinary catheters [22].

It has been suggested that antibacterial agents that target the bacterial membrane may be beneficial for the treatment of resistant infections, such as those caused by bacteria resident in biofilms, since such membrane-active agents typically retain the activity against metabolically inert bacteria [22,78]. Based on the excellent ability to disperse preformed biofilms of *P. aeruginosa* PAO1 and on the evidence of the time-kill assay, we have examined the effect of complex **1** on the mature *P. aeruginosa* PAO1 biofilm architecture by microscopy after Live/Dead staining, whereby intact living cells appeared green and dead cells appeared red (Fig. 3c). The biofilms were formed for 24 h on the glass cover slips, and their

disruption was induced for 24 h in the presence of 10 and 20 μg/mL (11.6 and 23.2 μM) of complex **1**. After the treatment, the biofilms exhibited a less established architecture, and most cells were sparsely scattered on the glass surface in a thin monolayer, detected as green or red single bacteria, compared to the non-treated control, which appear mature and densely stacked in multi-cell layers, demonstrated by large areas of double positive orange staining (Fig. 3c). It follows that the silver(I) complexes not only inhibited biofilm formation but also facilitated cell detachment from the mature preformed biofilms. Similarly, $AgNO_3$ was found to be able to inhibit the growth of *Staphylococcus aureus* at concentrations similar to determined MIC values for rapidly growing free cultures; however, elimination of the mature biofilms was achieved [78].

3.4. In vitro DNA interaction and molecular docking

The binding interaction of transition metal complexes with DNA is of interest for both therapeutic and scientific reasons [91-93]. The silver(I) compounds **1**-**5** have the ability to competitively intercalate double stranded bacterial genomic DNA, which results in the inability of ethidum bromide to intercalate and emit under UV exposure (Fig. 4). Ethidium bromide is one of the most sensitive fluorescence probes for DNA binding: intercalation of a substrate into DNA leads to a decrease in the fluorescence intensity of the ethidium bromide-DNA complex. From the reduced emission intensity, visualized by gel electrophoresis, the most stable intercalation occurred with **4** and $AgNO_3$ (100%), while other compounds intercalated between 20% and 92% relative to the DMSO control (Fig. 4). The capacity of the silver(I) complexes to interact with DNA under the tested conditions followed the order **4** > **5** > **3** > **2** > **1**, and the order with the silver(I) salts was

$AgNO_3$ > $AgBF_4$ > $AgClO_4 \cdot xH_2O$ > $AgCF_3SO_4$ (Fig. 4). This is in line with a mechanistic study of the antibacterial effect of silver ions on *E. coli* and *S. aureus*, carried out by electron microscopy combined with X-ray microanalysis using $AgNO_3$ [94]. That study suggested an antibacterial mechanism of silver(I) through primary DNA interaction, which caused the loss of its replication ability and a general inactivation of sulfur containing proteins. Similar binding effect of **4** and **5** in comparison to $AgNO_3$ suggest that DNA may be the primary target in the antibacterial mechanism of these two complexes, while this was not the case for **1**. Interestingly, complex **1** has monodentate nitrate and phthalazine as ligands (Fig. 1) and, as shown in time-kill assays, it may act on the membrane as the primary target. It is important to note that the molar ratio of silver(I) in $AgNO_3$ is more than 2-fold greater than in **1-5**. Therefore, we concluded that the interaction with DNA is not solely due to the presence of silver(I) ions and that the overall structure of the complexes plays a crucial role. The strong binding ability of **4** and **5** is correlated with excellent antibacterial properties (Table 3) and moderate cytotoxic levels (Table 4).

Fig. 4

Pyrimidine base pairs in DNA duplexes selectively capture metal ions to form metal ion mediated base pairs [52]. More specifically, cytosine-cytosine and thymine-thymine base pairs selectively capture silver(I) and mercury(II) ions, respectively, and the metallo-base pairs C-Ag(I)-C and T-Hg(II)-T are formed in DNA duplexes [93]. Transition metal complexes are known to bind to DNA via both covalent and non-covalent interactions. In covalent binding, the labile ligand of

a complex is replaced by a nitrogen base of DNA, such as guanine N7. Non-covalent DNA interactions include intercalative, electrostatic and groove (surface) binding of cationic metal complexes [52].

The investigation of DNA-metal complex interactions, the identification of the binding site (minor or major groove) and the prediction of binding affinities can be probed with molecular docking [58,95,96]. Therefore, a brief molecular docking study was carried out to gain in silico information about interactions of studied silver(I) complexes **1-5** with DNA. The best geometrical orientation inside DNA helix and the highest binding affinity with DNA helix were predicted using the top-ranking poses of studied complexes. The binding energy of the solution, softened attractive and repulsive van der Waals energy, atomic contact energy and insideness measure were used as scoring functions for binding affinity assessment (Table S2). Top-ranked poses according to used scoring functions are presented in Fig. S7.

According to all calculated values for scoring functions related to the highest binding activity has metal complex **5**, followed by complexes **3** and **4**. This was in reasonable good agreement with the experimental results obtained when bacterial gDNA was used as substrate (Fig. 4). The minimum energy docked pose revealed that all complexes very well fitted into the DNA minor groove. Docking poses suggested that silver(I) complexes and DNA base pairs were arranged in such a way that they have effective π-π stacking interactions. These interactions could lead to higher van der Waals interaction with the DNA functional groups which define the stability of groove, making the AT regions more preferable regions of dodecamer [97].

4. Conclusions

In this study five silver(I) complexes with aromatic nitrogen-containing heterocycles, phthalazine (phtz) and quinazoline (qz), have been synthesized and characterized by using different spectroscopic and single-crystal X-ray diffraction techniques. In the reaction between AgX salts (X = NO_3^-, $CF_3SO_3^-$ and ClO_4^-) and phtz only dinuclear silver(I) complexes of the general formula {[Ag(X-*O*)(phtz-*N*)]$_2$(μ-phtz-*N,N'*)$_2$} are formed, while the reaction with qz ligand results in the formation of polynuclear complexes, {[Ag(CF_3SO_3-*O*)(qz-*N*)]$_2$}$_n$ and {[Ag(qz-*N*)][BF_4]}$_n$. The investigation of the antimicrobial properties of these silver(I) complexes shows that they are efficient against pathogenic *P. aeruginosa* and have a marked ability to disrupt preformed biofilms of its clinical isolates with high inherent resistance to antibiotics. Given the improved therapeutic potential in comparison to clinically used $AgNO_3$, silver(I) complexes with phthalazine and quinazoline have a great potential for the treatment of a variety of microbial pathogens such as *P. aeruginosa* that are not easily destroyed by routine antibiotics.

Abbreviations

phtz	phthalazine
qz	quinazoline
MIC	minimum inhibitory concentration
MRC5	human lung fibroblastic cell line
P. aeruginosa	*Pseudomonas aeruginosa*
CF	cystic fibrosis
N-heterocycles	aromatic nitrogen-containing heterocycles
DMSO	dimethyl sulfoxide
NMR spectroscopy	nuclear magnetic resonance spectroscopy
IR spectroscopy	infrared spectroscopy
UV-vis spectrophotometry	ultraviolet-visible spectrophotometry
adp	atomic displacement parameter
NCTC	national collection of type cultures
ATCC	american type culture collection
P. aeruginosa MD-49 and MD-50	*Pseudomonas aeruginosa* clinical isolates
cfu	colony forming units

LB broth	Luria-Bertani broth
TSB	tryptic soy broth
PBS	phosphate buffered saline
PI	propidium iodide
MTT	3-(4,5-dimethylthiazol-2-yl)-2,5-diphenyltetrazolium bromide
RPMI-1640	Roswell Park Memorial Institute medium
FBS	fetal bovine serum
IC_{50}	concentration of the compound inhibiting growth by 50%
gDNA	genomic DNA
TAE buffer	tris acetate EDTA buffer
PDB	protein data bank
NTf_2^-	triflimide anion
terpy	2,2':6',2''-terpyridine
E. coli	*Enterococcus faecalis*
S. aureus	*Staphylococcus aureus*
E. faecalis	*Enterococcus faecalis*
C. albicans	*Candida albicans*
WI-38	human fibroblastic cell line
L-929	murine fibroblastic cell line
C	cytosine
T	thymine
A	adenosine

Acknowledgements

This work has been financially supported by the Ministry of Education and Science, Republic of Serbia, under Grant No. 172036 and 173048. B.Đ.G. gratefully acknowledges financial support from the German Academic Exchange Service (DAAD) during postdoctoral stay at the University of Heidelberg, Germany.

Dr. Željko Vitnik (Department of Chemistry, IchTM - Institute of Chemistry, Technology and Metallurgy, University of Belgrade, Belgrade, Serbia) is greatly acknowledged for providing the Gaussian 09 and computing facilities. Dr. Dusan Misic (Faculty of Veterinary Medicine, University of Belgrade) is acknowledged for supplying clinical isolates.

Appendix A. Supplementary data

Supplementary Material associated with this article includes Figs. S1-S7 and Tables S1 and S2. CCDC 1408426-1408430 contains the supplementary crystallographic data for **1**-**5**. These data can be obtained free of charge viahttp://www.ccdc.cam.ac.uk/conts/retrieving.html, or from the Cambridge Crystallographic Data Centre, 12 Union Road, Cambridge CB2 1EZ, UK; fax: (+44) 1223-336-033; or e-mail: deposit@ccdc.cam.ac.uk.

References

[1] S. Harbarth, U. Theuretzbacher, J. Hackett, J. Antimicrob. Chemother. 70 (2015) 1604-1607.

[2] A. Penesyan, M. Gillings, I.T. Paulsen, Molecules 20 (2015) 5286-5298.

[3] N. Høiby, Pathog. Dis. 70 (2014) 205-211.

[4] N. Høiby, T. Bjarnsholt, M. Givskov, S. Molin, O. Ciofu, Int. J. Antimicrob. Agents 35 (2010) 322-332.

[5] L. Yang, Y. Liu, H. Wu, Z. Song, N. Høiby, S. Molin, M. Givskov, FEMS Immunol. Med. Microbiol. 65 (2012) 146-157.

[6] N. Høiby, T. Bjarnsholt, C. Moser, G.L. Bassi, T. Coenye, G. Donelli, L. Hall-Stoodley, V. Holá, C. Imbert, K. Kirketerp-Møller, D. Lebeaux, A. Oliver, A.J. Ullmann, C. Williams, Clin. Microbiol. Infect. (2015) doi:10.1016/j.cmi.2014.10.024.

[7] T. Bjarnsholt, M. Givskov, Anal. Bioanal. Chem. 387 (2007) 409-414.

[8] K. Olejnickova, V. Hola, F. Ruzicka, Pathog. Dis. 72 (2014) 87-94.

[9] D. Savoia, Future Microbiol. 9 (2014) 917-928.

[10] J. Kim, J.S. Hahn, M.J. Franklin, P.S. Stewart, J. Yoon, J. Antimicrob. Chemother. 63 (2009) 129-135.

[11] G. Laverty, S.P. Gorman, B.F. Gilmore, Pathogens 3 (2014) 596-632.

[12] T. Tolker-Nielsen, APMIS Supplementum (2014) 1-51.

[13] S.H. van Rijt, P.J. Sadler, Drug Discov. Today, 14 (2009) 1089-1097.

[14] S. Eckhardt, P.S. Brunetto, J. Gagnon, M. Priebe, B. Giese, K.M. Fromm, Chem. Rev. 113 (2013) 4708-4754.

[15] E. Alessio (Ed.), Bioinorganic Medicinal Chemistry, Wiley-VCH Verlag GmbH & Co. KGaA, Wienheim, 2011.

[16] S. Medici, M. Peana, V.M. Nurchi, J.I. Lachowicz, G. Crisponi, M.A. Zoroddu, Coord. Chem. Rev. 284 (2015) 329-350 and references cited therein.

[17] B.Đ. Glišić, M.I. Djuran, Dalton Trans. 43 (2014) 5950-5969.

[18] H.J. Klasen, Burns 26 (2000) 117-130.

[19] R.B.-K. Wakshlak, R. Pedahzur, D. Avnir, Sci. Rep. 5 (2015) doi:10.1038/srep09555.

[20] J.A. Lemire, J.J. Harrison, R.J. Turner, Nat. Rev. Microbiol. 11 (2013) 371-384.

[21] W.-R. Li, X.-B. Xie, Q.-S. Shi, H.-Y. Zeng, Y.-S. OU-Yang, Y.-B. Chen, Appl. Microbiol. Biotechnol. 85 (2010) 1115-1122.

[22] T. Bjarnsholt, K. Kirketerp-Møller, S. Kristiansen, R. Phipps, A.K. Nielsen, P.Ø. Jensen, N. Høiby, M. Givskov, APMIS 115 (2007) 921-928.

[23] J. Liu, D.A. Sonshine, S. Shervani, R.H. Hurt, ACS Nano 4 (2010) 6903-6913.

[24] U. Kalinowska-Lis, A. Felczak, L. Chęcińska, K. Lisowska, J. Ochocki, J. Organomet. Chem. 749 (2014) 394-399.

[25] L. Ortego, J. Gonzalo-Asensio, A. Laguna, M.D. Villacampa, M.C. Gimeno, J. Inorg. Biochem. 146 (2015) 19-27.

[26] C. Pettinari, F. Marchetti, G. Lupidi, L. Quassinti, M. Bramucci, D. Petrelli, L.A. Vitali, M.F.C.G. da Silva, L.M.D.R.S. Martins, P. Smoleński, A.J. Pombeiro, Inorg. Chem. 50 (2011) 11173-11183.

[27] R. Rowan, T. Tallon, A.M. Sheahan, R. Curran, M. McCann, K. Kavanagh, M. Devereux, V. McKee, Polyhedron 25 (2006) 1771-1778.

[28] H.S. Carr, T.J. Wlodkowski, H.S. Rosenkranz, Antimicrob. Agents Chemother. 4 (1973) 585-587.

[29] S. Ray, R. Mohan, J.K. Singh, M.K. Samantaray, M.M. Shaikh, D. Panda, P. Ghosh, J. Am. Chem. Soc. 129 (2007) 15042-15053.

[30] T. Storr, K.H. Thompson, C. Orvig, Chem. Soc. Rev. 35 (2006) 534-544.

[31] K. Nomiya, A. Yoshizawa, K. Tsukagoshi, N.C. Kasuga, S. Hirakawa, J. Watanabe, J. Inorg. Biochem. 98 (2004) 46-60.

[32] B.Đ. Glišić, B. Warżajtis, N.S. Radulović, U. Rychlewska, M.I. Djuran, Polyhedron 87 (2015) 208-214.

[33] G.K. Patra, I. Goldberg, S. De, D. Datta, CrystEngComm 9 (2007) 828-832.

[34] SAINT, Bruker AXS GmbH, Karlsruhe, Germany, 1997-2013.

[35] R.H. Blessing, Acta Crystallogr. Sect. A: Found. Crystallogr. 51 (1995) 33-38.

[36] G.M. Sheldrick, SADABS, Bruker AXS GmbH, Karlsruhe, Germany 2004-2014.

[37] L. Krause, R. Herbst-Irmer, G.M. Sheldrick, D. Stalke, J. Appl. Crystallogr. 48 (2015) 3-10.

[38] G.M. Sheldrick, TWINABS, Bruker AXS GmbH, Karlsruhe, Germany 2004-2012.

[39] L. Palatinus, SUPERFLIP, EPF Lausanne, Switzerland, 2007-2014.

[40] L. Palatinus, G. Chapuis, J. Appl. Crystallogr. 40 (2007) 786-790.

[41] G.M. Sheldrick, SHELXL-20xx, University of Göttingen and Bruker AXS GmbH, Karlsruhe, Germany 2012-2014.

[42] G.M. Sheldrick, Acta Crystallogr. Sect. A: Found. Crystallogr. 64 (2008) 112-122.

[43] G.M. Sheldrick, Acta Crystallogr. Sect. C: Cryst. Struct. Commun. 71 (2015) 3-8.

[44] I.J. Bruno, J.C. Cole, P.R. Edgington, M. Kessler, C.F. Macrae, P. McCabe, J. Pearson, R. Taylor, Acta Crystallogr. Sect. B: Struct. Sci. 58 (2002) 389-397.

[45] J.T. Casey, C. O'Cleirigh, P.K. Walsh, D.G. O'Shea, J. Microbiol. Meth. 58 (2004) 327-334.

[46] J.H. Merritt, D.E. Kadouri, G.A. O'Toole, Current protocols in microbiology, chapter 1, unit 1B.1, 2005.

[47] N. Barraud, J.A. Moscoso, J.M. Ghigo, A. Filloux, Methods Mol. Biol. 1149 (2014) 643-651.

[48] D.G. Ha, S.L. Kuchma, G.A. O'Toole, Methods Mol. Biol. 1149 (2014) 67-72.

[49] D.G. Ha, S.L. Kuchma, G.A. O'Toole, Methods Mol. Biol. 1149 (2014) 59-65.

[50] M.B. Hansen, S.E. Nielsen, K. Berg, J. Immunol. Methods 119 (1989) 203-210.

[51] P. Smoleński, S.W. Jaros, C. Pettinari, G. Lupidi, L. Quassinti, M. Bramucci, L.A. Vitali, D. Petrelli, A. Kochel, A.M. Kirillov, Dalton Trans. 42 (2013) 6572-6581.

[52] V.T. Yilmaz, E. Gocmen, C. Icsel, M. Cengiz, S.Y. Susluer, O. Buyukgungor, J. Photochem. Photobiol. B 131 (2014) 31-42.

[53] E.A. Amin, D.G. Truhlar, J. Chem. Theory Comput. 4 (2008) 75-85.

[54] G. Frison, G. Ohanessian, J. Comput. Chem. 29 (2008) 416-433.

[55] J.J.P. Stewart, J. Mol. Model. 13 (2007) 1173-1213.

[56] M.J. Frisch, G.W. Trucks, H.B. Schlegel, G.E. Scuseria, M.A. Robb, J. Cioslowski, D. J. Fox, Gaussian, Inc.: Wallingford, CT, 2004.

[57] H.R. Drew, R.M. Wing, T. Takano, C. Broka, S. Tanaka, K. Itakura, R.E. Dickerson, Proc. Natl. Acad. Sci. USA 78 (1981) 2179-2183.

[58] L. Senerovic, M.D. Zivkovic, A. Veselinovic, A. Pavic, M.I. Djuran, S. Rajkovic, J. Nikodinovic-Runic, J. Med. Chem. 58 (2015) 1442-1451.

[59] K. Suntharalingam, O. Mendoza, A.A. Duarte, D.J. Mann, R. Vilar, Metallomics 5 (2013) 514−523.

[60] D. Schneidman-Duhovny, Y. Inbar, R. Nussinov, H.J. Wolfson, Nucleic Acids Res. 33 (2005) W363-W367.

[61] E. Mashiach, D. Schneidman-Duhovny, N. Andrusier, R. Nussinov, H.J. Wolfson, Nucleic Acids Res. 36 (2008) W229-W232.

[62] L. Yang, D.R. Powell, R.P. Houser, Dalton Trans. (2007) 955-964.

[63] D.L. Reger, E.A. Foley, M.D. Smith, Inorg. Chem. 49 (2010) 234-242.

[64] D.L. Reger, R.P. Watson, J.R. Gardinier, M.D. Smith, Inorg. Chem. 43 (2004) 6609-6619.

[65] A. Melaiye, Z. Sun, K. Hindi, A. Milsted, D. Ely, D.H. Reneker, C.A. Tessier, W.J. Youngs, J. Am. Chem. Soc. 127 (2005) 2285-2291.

[66] A. Bondi, J. Phys. Chem. 68 (1964) 441-452.

[67] N.C. Baenziger, A.W. Struss, Inorg. Chem. 15 (1976) 1807-1809.

[68] D.R. Whitcomb, R.D. Rogers, J. Chem. Crystallogr. 25 (1995) 137-142.

[69] Y.E. Türkmen, S. Sen, V.H. Rawal, CrystEngComm 15 (2013) 4221-4224.

[70] A. Tăbăcaru, C. Pettinari, F. Marchetti, C. di Nicola, K.V. Domasevitch, S. Galli, N. Masciocchi, S. Scuri, I. Grappasonni, M. Cocchioni, Inorg. Chem. 51 (2012) 9775-9788.

[71] A.B.P. Lever, E. Mantovani, B.S. Ramaswamy, Can. J. Chem. 49 (1971) 1957-1964.

[72] D. Johnston, D.F. Shriver, Inorg. Chem. 32 (1993) 1045-1047.

[73] M.R. Rosenthal, J. Chem. Educ. 50 (1973) 331-335.

[74] A.M. Petrosyan, Vib. Spectrosc. 43 (2007) 284-289.

[75] B.Đ. Glišić, Z.D. Stanić, S. Rajković, V. Kojić, G. Bogdanović, M.I. Djuran, J. Serb. Chem. Soc. 78 (2013) 1911-1924.

[76] J.-A. Zhang, M. Pan, J.-Y. Zhang, H.-K. Zhang, Z.-J. Fan, B.-S. Kang, C.-Y. Su, Polyhedron 28 (2009) 145-149.

[77] G. Humphreys, G.L. Lee, S.L. Percival, A.J. McBain, J. Antimicrob. Chemother. 66 (2011) 2556-2561.

[78] C.P. Randall, L.B. Oyama, J.M. Bostock, I. Chopra, A.J. O'Neill, J. Antimicrob. Chemother. 68 (2013) 131-138.

[79] M.A.M. Abu-Youssef, V. Langer, L. Öhrström, Dalton Trans. (2006) 2542-2550.

[80] P. Kleyi, R.S. Walmsley, M.A. Fernandes, N. Torto, Z.R. Tshentu, Polyhedron 41 (2012) 25-29.

[81] U. Kalinowska-Lis, A. Felczak, L. Chęcińska, K. Zawadzka, E. Patyna, K. Lisowska, J. Ochocki, Dalton Trans. 44 (2015) 8178-8189.

[82] M. McCann, B. Coyle, J. Briody, F. Bass, N. O'Gorman, M. Devereux, K. Kavanagh, V. McKee, Polyhedron 22 (2003) 1595-1601.

[83] N.C. Kasuga, Y. Takagi, S.-I. Tsuruta, W. Kuwana, R. Yoshikawa, K. Nomiya, Inorg. Chim. Acta 368 (2011) 44-48.

[84] R.A. Khan, K. Al-Farhan, A. de Almeida, A. Alsalme, A. Casini, M. Ghazzali, J. Reedijk, J. Inorg. Biochem. 140 (2014) 1-5.

[85] C.N. Banti, S.K. Hadjikakou, Metallomics 5 (2013) 569-596.

[86] I. Chevrier, J.L. Sagué, P.S. Brunetto, N. Khanna, Z. Rajacic, K.M. Fromm, Dalton Trans. 42 (2013) 217-231.

[87] G.A. O'Toole, R. Kolter, Mol. Microbiol. 28 (1998) 449-461.

[88] G.A. O'Toole, R. Kolter, Mol. Microbiol. 30 (1998) 295-304.

[89] J.L. Fothergill, C. Winstanley, C.E. James, Expert Rev. Anti. Infect. Ther. 10 (2012) 219-235.

[90] N. Høiby, O. Ciofu, H.K. Johansen, Z.J. Song, C. Moser, P.Ø. Jensen, S. Molin, M. Givskov, T. Tolker-Nielsen, T. Bjarnsholt, Int. J. Oral Sci. 3 (2011) 55-65.

[91] R.S. Kumar, S. Arunachalam, Eur. J. Med. Chem. 44 (2009) 1878-1883.

[92] S. Mandal, A. Hepp, J. Müller, Dalton Trans. 44 (2015) 3540-3543.

[93] A. Ono, H. Torigoe, Y. Tanaka, I. Okamoto, Chem. Soc. Rev. 40 (2011) 5855-5866.

[94] Q.L. Feng, J. Wu, G.Q. Chen, F.Z. Cui, T.N. Kim, J.O. Kim, J. Biomed. Mater. Res. 52 (2000) 662-668.

[95] P.A. Holt, J.B. Chaires, J. Trent, J. Chem. Inf. Model. 48 (2008) 1602−1615.

[96] G.L. Warren, C.W. Andrews, A.-M. Capelli, B. Clarke, J. LaLonde, M.H. Lambert, M. Lindvall, N. Nevins, S.F. Semus, S. Senger, G. Tedesco, I.D. Wall, J.M. Woolven, C.E. Peishoff, M.S. Head, J. Med. Chem. 49 (2006) 5912−5931.

[97] R. Filosa, A. Peduto, S. Di Micco, P. de Caprariis, M. Festa, A. Petrella, G. Capranico, G. Bifulco, Bioorg. Med. Chem. 17 (2009) 13−24.

Table and Figure Captions

Table 1

Selected bond distances (Å) and valence angles (°) in phthalazine-silver(I) complexes **1-3**.

Table 2

Selected bond distances (Å) and valence angles (°) in quinazoline-silver(I) complexes **4** and **5**.

Table 3

Antimicrobial activities of the investigated silver(I) complexes, silver(I) salts and *N*-heterocyclic ligands as MIC concentrations (μM).

Table 4

Antiproliferative effect of silver(I) complexes **1-5**, silver(I) salts and the *N*-heterocyclic ligands as IC_{50} concentrations (μM).

Table 5

The effect of silver(I) compounds in sub MIC concentrations (0.5 MIC) on the motility (swimming, twitching and swarming) of *P. aeruginosa* strains.

Scheme 1. Schematic presentation of the synthesis of silver(I) complexes with **(a)** phthalazine (phtz, **1-3**) and **(b)** quinazoline (qz, **4** and **5**). Numbering scheme of carbon atoms in phtz and qz is in agreement with IUPAC recommendations for fused ring systems and does not match the one applied in the X-ray of silver(I) complexes with these ligands.

Fig. 1. Molecular structures of {[Ag(NO_3-*O*)(phtz-*N*)]$_2$(μ-phtz-*N,N'*)$_2$} (**1**), {[Ag(CF_3SO_3-*O*)(phtz-*N*)]$_2$(μ-phtz-*N,N'*)$_2$} (**2**) and {[Ag(ClO_4-*O*)(phtz-*N*)]$_2$(μ-phtz-*N,N'*)$_2$} (**3**). Only one of the two independent moieties of **2** is shown. Displacement

ellipsoids are drawn at 50% probability level and H atoms are represented by spheres of arbitrary size.

Fig. 2. The asymmetric units of polymeric $\{[Ag(CF_3SO_3\text{-}O)(qz\text{-}N)]_2\}_n$ (**4**) and $\{[Ag(qz\text{-}N)][BF_4]\}_n$ (**5**) complexes. Displacement ellipsoids are drawn at 50% probability level and H atoms are represented by spheres of arbitrary size.

Fig. 3. Biofilm formation **(a)** and disruption **(b)** by silver(I) compounds in *Pseudomonas aeruginosa* PAO1 (□), MD-49 (▣) and MD-50 (■). **(c)** Representative fluorescent microscopy image of a PAO1 mature biofilm, treated with 10 μg/mL (11.6 μM) and 20 μg/mL (23.2 μM) of complex **1**. (Bar represents 10 μm).

Fig. 4. In vitro interaction of the silver(I) complexes and salts with genomic DNA (gDNA) from *P. aeruginosa* PAO1 (results are considered significant when compared to the DMSO control: ***$p<0.001$ and **$p<0.01$).

Table 1. Selected bond distances (Å) and valence angles (^{o}) in phthalazine-silver(I) complexes **1**-**3**.

1		**2**		**3**	
Ag—O1A	2.576(4)	Ag1/Ag51—O1/O51	2.533(2)/2.560(2)	Ag—O1	2.642(2)
Ag—N1	2.278(1)	Ag1/Ag51—N1/N51	2.283(2)/2.267(2)	Ag—N1	2.251(2)
Ag—N3	2.256(1)	Ag1/Ag51—N3/N53	2.346(2)/2.331(2)	Ag—N3	2.254(2)
Ag—N4^{i}	2.306(1)	Ag1/Ag51—N4/N54	2.266(2)/2.256(2)	Ag—N4	2.317(2)
N4—Ag^{i}	2.306(1)			Ag—O1	2.624(2)
N1—Ag—O1A	95.22(5)	N1/N51—Ag1/Ag51—O1/O51	100.55(5)/102.12(5)	N1—Ag—O1	112.70(5)
N1—Ag—N4^{i}	106.07(4)	N1/N51—Ag1/Ag51—N4/N54^{ii}	128.00(5)/128.55(6)	N1—Ag—N4	107.34(6)
N3—Ag—O1A	92.69(5)	N3/N53—Ag1/Ag51—O1/O51	84.42(5)/90.64(6)	N3—Ag—O1	81.17(5)
N3—Ag—N1	123.74(5)	N3/N53—Ag1/Ag51—N1/N51	111.28(5)/106.79(6)	N3—Ag—N1	129.19(6)
N3—Ag—N4^{i}	124.13(4)	N3/N53—Ag1/Ag51—N4/N54	119.08(5)/123.19(5)	N3—Ag—N4	122.21(5)
N4^{i}—Ag—O1A	107.38(6)	N4/N54—Ag1/Ag51—O1/O51	96.42(6)/89.61(6)	N4—Ag—O1	88.28(6)
N5—O1A—Ag	111.6(2)	S1/S51—O1/O51—Ag1/Ag51	133.9(1)/124.32(9)	Cl—O1—Ag	120.36(8)
N2—N1—Ag	116.38(8)	N2/N52—N1/N51 —Ag1/Ag51	110.3(1)/112.9(1)	N2—N1—Ag	115.2(1)
C8—N1—Ag	122.80(9)	C8/C58—N1/N51—Ag1/Ag51	129.3(1)/125.8 (1)	C8—N1—Ag	124.3(1)
N4—N3—Ag	114.12(8)	N4^{ii}/N54—N3/N53—Ag1/Ag51	120.2(1)/117.8(1)	N4^{iii}—N3—Ag	117.2(1)
C9—N3—Ag	126.30(9)	C9/C59—N3/N53—Ag1/Ag51	119.3(1)/112.3(1)	C9—N3—Ag	123.0(1)
N3—N4—Ag^{i}	115.75(8)	N3^{ii}/N53—N4/N54—Ag1/Ag51	117.7(1)/113.2(1)	N3^{iii}—N4—Ag	118.0(1)
C16—N4—Ag^{i}	121.78(9)	C16^{ii}/C66—N4/N54—Ag1/Ag51^{ii}	122.4(1)/126.4(1)	C16^{iii} —N4—Ag	121.8(1)

Symmetry code(s): (i) -*x*+1, -*y*+1, -*z*; (ii)-*x*, -*y*, -*z*+1; (iii) -*x*+2, -*y*, -*z*+1

Table 2. Selected bond distances (Å) and valence angles (°) in quinazoline-silver(I) complexes **4** and **5**.

4		**5**	
Ag1—N1	2.195(2)	Ag1—N1	2.147(4)
Ag1—N4	2.207(2)	Ag1—N3	2.142(4)
Ag2—N2	2.201(2)	Ag2—N2	2.126(4)
Ag2—N3	2.191(2)	Ag2—N4^{ii}	2.141(4)
Ag2—O12	2.556(2)	N4—Ag2^{iii}	2.141(4)
Ag1—O21	2.742(2)		
N1—Ag1—N4	169.03(7)	N3—Ag1—N1	177.0(2)
N2—Ag2—O12	88.90(8)	N2—Ag2—N4^{ii}	172.7 (2)
N1—Ag1—O21	88.28(8)	C1—N1—Ag1	117.1(3)
N3—Ag2—O12	103.00(8)	C8—N1—Ag1	124.1(4)
N4—Ag1—O21	101.29(8)	C8—N1—C1	118.3(4)
		C1—N2—Ag2	116.9(3)
N3—Ag2—N2	168.02(7)	C1—N2—C2	118.4(4)
S1—O12—Ag2	114.0(1)	C2—N2—Ag2	124.1(3)
S2—O21—Ag1	97.4(1)	C9—N3—Ag1	116.0(3)
C1—N1—Ag1	120.2(2)	C16—N3—Ag1	125.5(4)
C8—N1—Ag1	122.6(2)	C16—N3—C9	118.0(4)
C8—N1—C1	117.1(2)	C9—N4—Ag2^{iii}	116.6(3)
C1—N2—Ag2	120.5(2)	C9—N4—C10	118.5(4)
C1—N2—C2	117.7(2)	C10—N4—Ag2^{iii}	124.9(3)
C2—N2—Ag2	121.6(2)		
C9—N3—Ag2	120.8(2)		
C16—N3—Ag2	121.8(2)		
C16—N3—C9	117.4(2)		
C9^{i}—N4—Ag1	121.0(2)		
C9^{i}—N4—C10^{i}	117.7(2)		
C10^{i} —N4—Ag1	120.6(2)		

Symmetry code(s): (i) *x*, *y*+1, *z*; (ii) *x*+1, *y*+1, *z*; (iii) *x*-1, *y*-1,

Table 3. Antimicrobial activities of the investigated silver(I) complexes, silver(I) salts and *N*-heterocyclic ligands as MIC concentrations (μM).

Compound	***Pseudomonas aeruginosa***			***Escherichia coli***	***Enterococcusfaecalis***	***Staphylococcus aureus***	***Candida albicans***
	PAO1	***DM-49***	***DM-50***				
				Silver(I) complexes			
1	2.9 ± 0.2	14.5 ± 0.3	9.1 ± 0.3	18.1 ± 0.3	29.1 ± 1.2	9.1 ± 0.3	58.1 ± 3.5
2	5.2 ± 0.1	24.2 ± 0.5	9.7 ± 0.6	19.3 ± 0.4	19.3 ± 1.0	15.1 ± 0.2	48.3 ± 3.9
3	7.6 ± 0.2	13.4 ± 0.4	13.4 ± 0.4	13.4 ± 0.2	16.7 ± 0.5	8.3 ± 0.2	53.5 ± 6.4
4	12.1 ± 0.3	8.0 ± 0.3	8.0 ± 0.3	16.1 ± 0.4	25.8 ± 0.9	12.1 ± 0.4	64.6 ± 3.9
5	28.9 ± 0.9	19.1 ± 0.9	15.4 ± 0.9	28.9 ± 0.9	48.0 ± 0.9	26.2 ± 1.2	77.0 ± 3.1
				Silver(I) salts			
$AgNO_3$	18.2 ± 0.6	36.5 ± 1.2	29.4 ± 0.6	45.9 ± 0.6	58.9 ± 3.5	18.2 ± 0.6	294.3 ± 17.7
$AgCF_3SO_3$	21.0 ± 0.8	24.1 ± 0.8	13.6 ± 0.8	48.6 ± 0.4	30.4 ± 0.8	21.0 ± 0.8	97.3 ± 3.9
$AgBF_4$	7.7 ± 0.5	12.8 ± 0.5	15.9 ± 0.5	27.7 ± 0.5	80.1 ± 1.5	15.9 ± 1.0	256.8 ± 15.4
$AgClO_4 \cdot xH_2O$	24.6 ± 1.0	60.3 ± 1.0	26.5 ± 1.0	41.0 ± 0.5	48.2 ± 2.9	26.0 ± 1.0	602.9 ± 19.3
				N-heterocyclic ligands			
phthalazine	3841.7 ± 76.8	1920.9 ± 30.7	3841.7 ± 76.8	1920.9 ± 30.7	3841.7 ± 76.8	1920.9 ± 30.7	3841.7 ± 76.8
quinazoline	3841.7 ± 76.8	1920.9 ± 30.7	3841.7 ± 76.8	1920.9 ± 30.7	3841.7 ± 76.8	1920.9 ± 30.7	3841.7 ± 76.8

Table 4. Antiproliferative effect of silver(I) complexes **1-5,** silver(I) salts and the *N*-heterocyclic ligands as IC_{50} concentrations (μM).

Compound	MRC5 cells IC_{50}[a]
1	20.9 ± 1.2
2	9.7 ± 0.9
3	3.2 ± 0.2
4	12.3 ± 0.6
5	24.6 ± 0.9
$AgNO_3$	8.8 ± 0.6
$AgCF_3SO_3$	8.2 ± 0.8
$AgBF_4$	6.2 ± 0.5
$AgClO_4 \cdot xH_2O$	5.8 ± 1.0
phthalazine[b]	768.3± 38.4
quinazoline[b]	768.3± 38.4

[a]IC_{50} is defined as the concentration inhibiting 50% of cell growth after the treatment with the test compounds. Results are from three independent experiments, each performed in triplicate.
[b]No dose dependence

Table 5. The effect of silver(I) compounds in sub MIC concentrations (0.5 MIC) on the motility (swimming, twitching and swarming) of *P. aeruginosa* strains.

Silver(I) compound	PAO1	MD-49	MD-50	PAO1	MD-49	MD-50	PAO1	MD-49	MD-50
	swimming			*twitching*			*swarming*		
1	64.0	79.8	100[a]	79.6	100	81.0	69.4	81.0	100
2	0[b]	64.1	100	65.7	39.5	76.6	100	64.0	100
3	11.1	75.1	100	65.7	51.1	60.1	100	64.2	100
4	44.4	0	100	0	13.8	49.0	100	64.4	100
5	84.1	0	100	0	8.2	42.3	100	25.5	100
$AgNO_3$	56.2	0	0	57.3	0	0.3	100	64.0	49.0
$AgCF_3SO_3$	56.3	87.1	100	0	18.4	0.5	100	100	100
$AgBF_4$	0	87.1	100	0	8.2	14.1	0	49.0	100
$AgClO_4 \cdot xH_2O$	0	87.1	0	0	23.6	0.5	17.3	36.3	64.4

[a]No significant difference observed in comparison to no treatment control. Results are an average of two independent experiments.

[b]No motility and reduced growth observable under tested conditions.

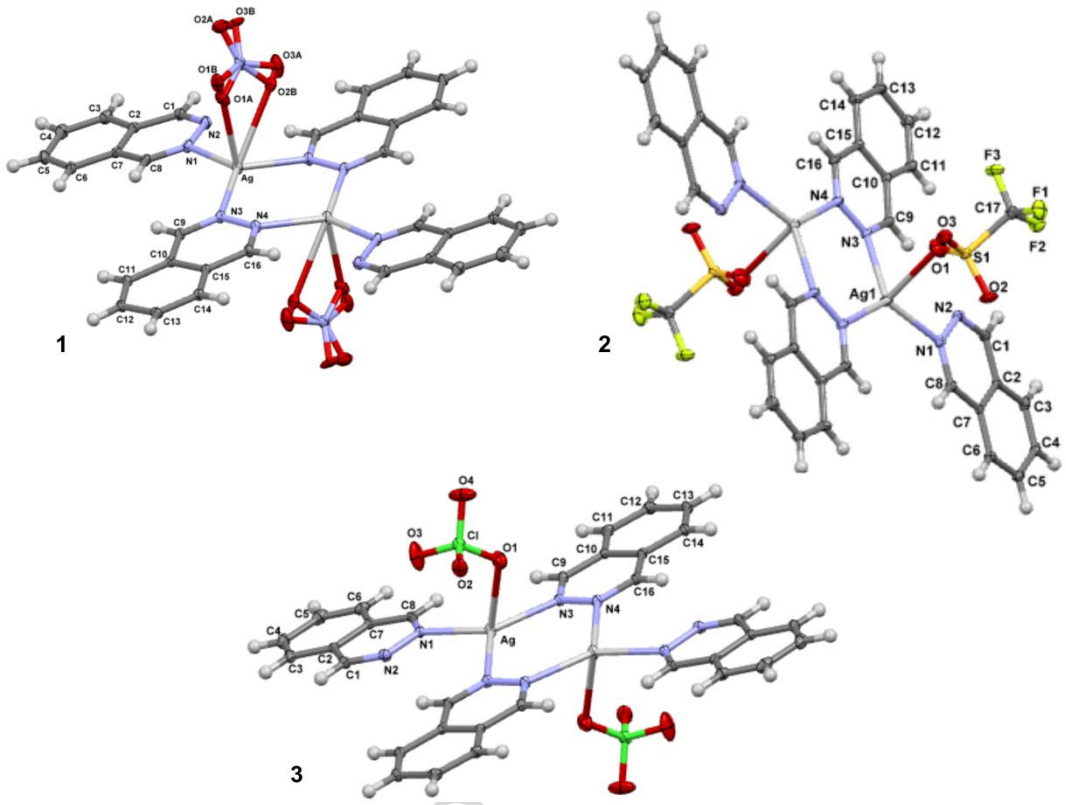

Fig. 1. Molecular structures of {[Ag(NO_3-*O*)(phtz-*N*)]$_2$(μ-phtz-*N,N'*)$_2$} (**1**), {[Ag(CF_3SO_3-*O*)(phtz-*N*)]$_2$(μ-phtz-*N,N'*)$_2$} (**2**) and {[Ag(ClO_4-*O*)(phtz-*N*)]$_2$(μ-phtz-*N,N'*)$_2$} (**3**). Only one of the two independent moieties of **2** is shown. Displacement ellipsoids are drawn at 50% probability level and H atoms are represented by spheres of arbitrary size.

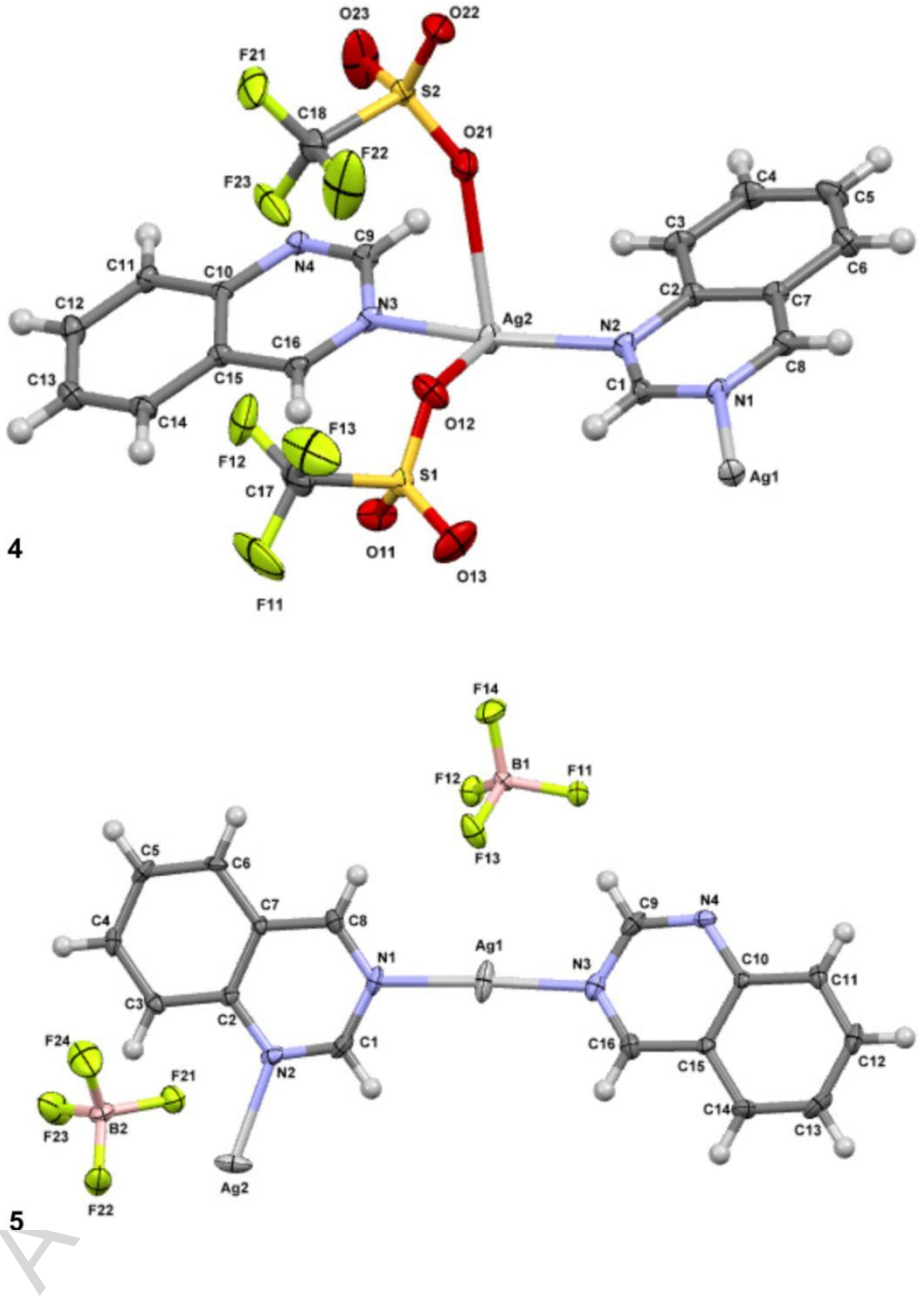

Fig. 2. The asymmetric units of polymeric $\{[Ag(CF_3SO_3\text{-}O)(qz\text{-}N)]_2\}_n$ (**4**) and $\{[Ag(qz\text{-}N)][BF_4]\}_n$ (**5**) complexes. Displacement ellipsoids are drawn at 50% probability level and H atoms are represented by spheres of arbitrary size.

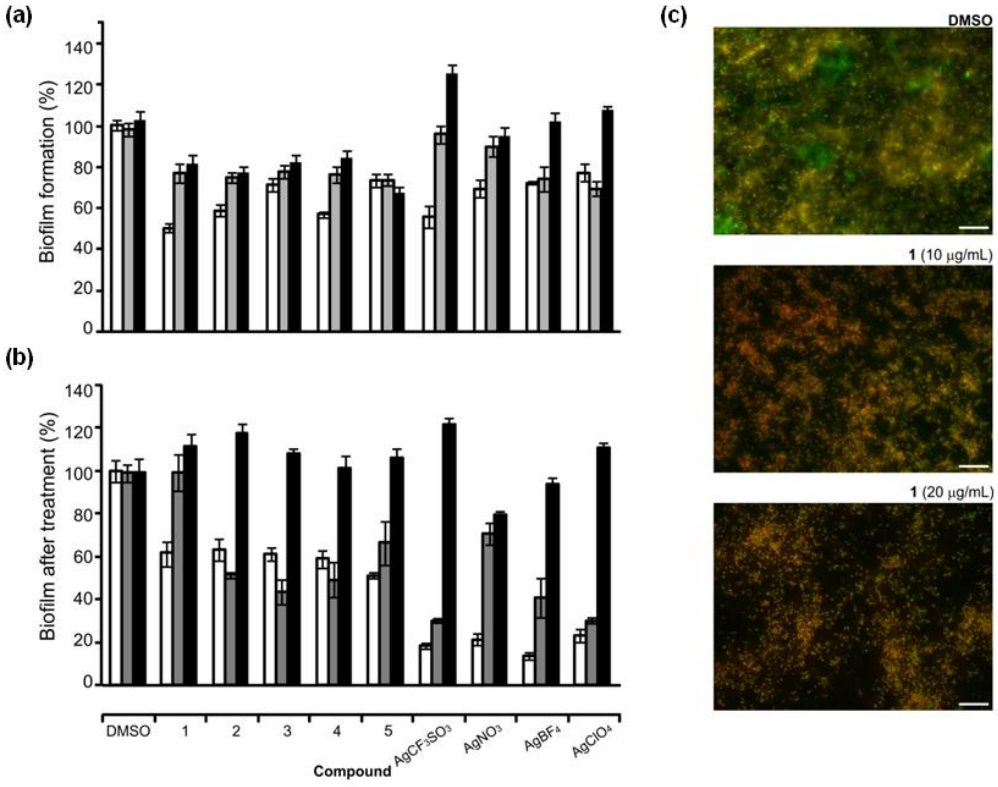

Fig. 3. Biofilm formation **(a)** and disruption **(b)** by silver(I) compounds in *Pseudomonas aeruginosa* PAO1 (□), MD-49 (▩) and MD-50 (■). **(c)** Representative fluorescent microscopy image of a PAO1 mature biofilm, treated with 10 μg/mL (11.6 μM) and 20 μg/mL (23.2 μM) of complex **1**. (Bar represents 10 μm).

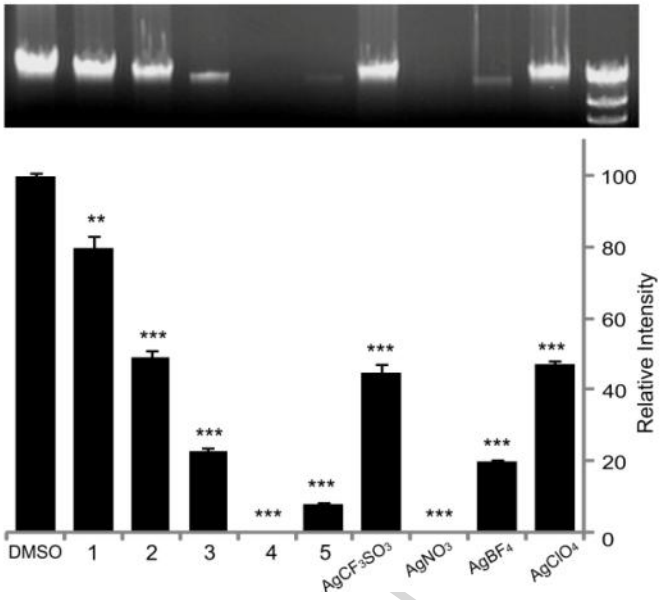

Fig. 4. In vitro interaction of the silver(I) complexes and salts with genomic DNA (gDNA) from *P. aeruginosa* PAO1 (results are considered significant when compared to the DMSO control: ***$p<0.001$ and **$p<0.01$).

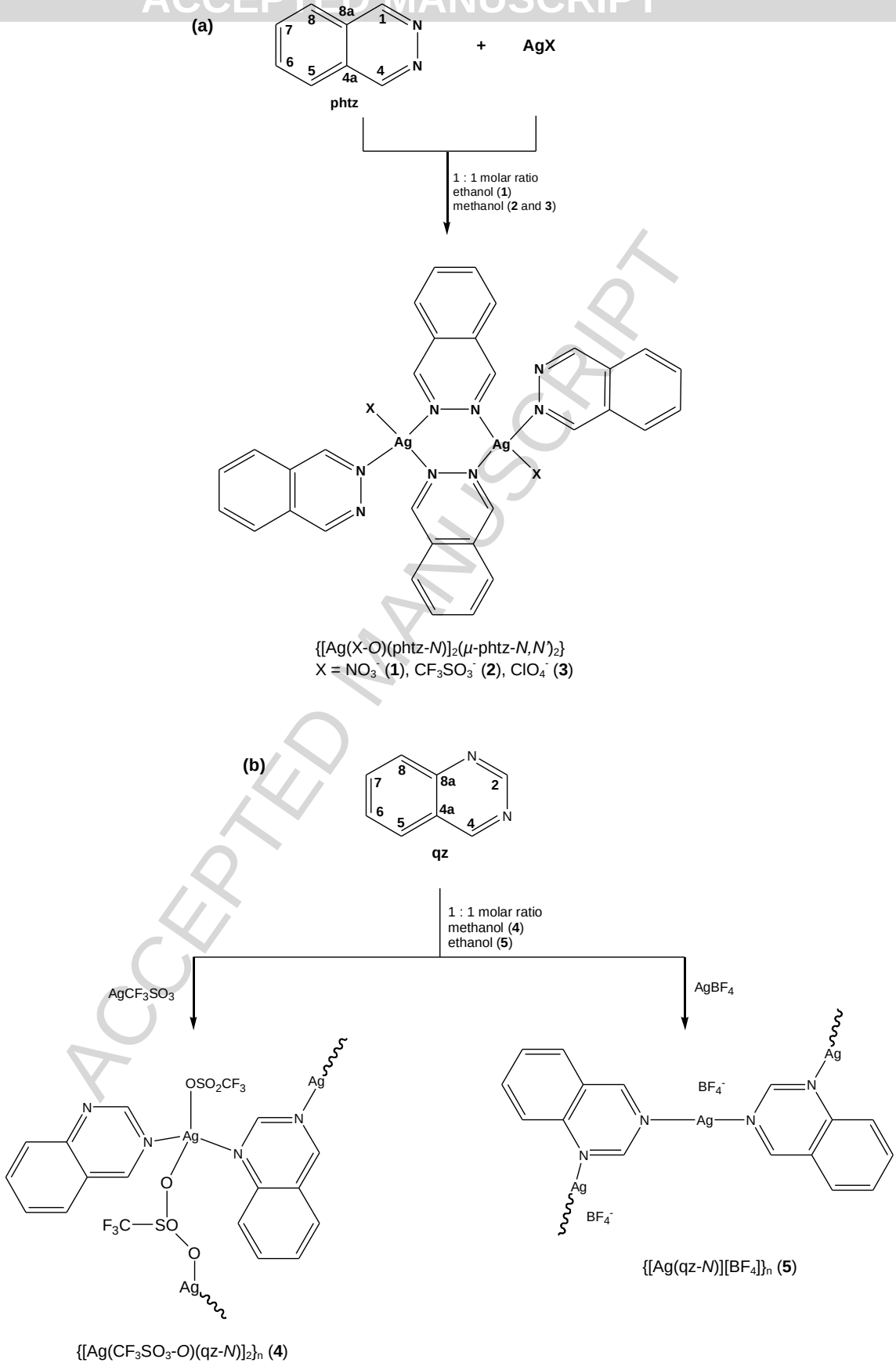

Scheme 1. Schematic presentation of the synthesis of silver(I) complexes with **(a)** phthalazine (phtz, **1-3**) and **(b)** quinazoline (qz, **4** and **5**). Numbering scheme of carbon atoms in phtz and qz is in agreement with IUPAC recommendations for fused ring systems and does not match the one applied in the X-ray of silver(I) complexes with these ligands.

Graphical abstract

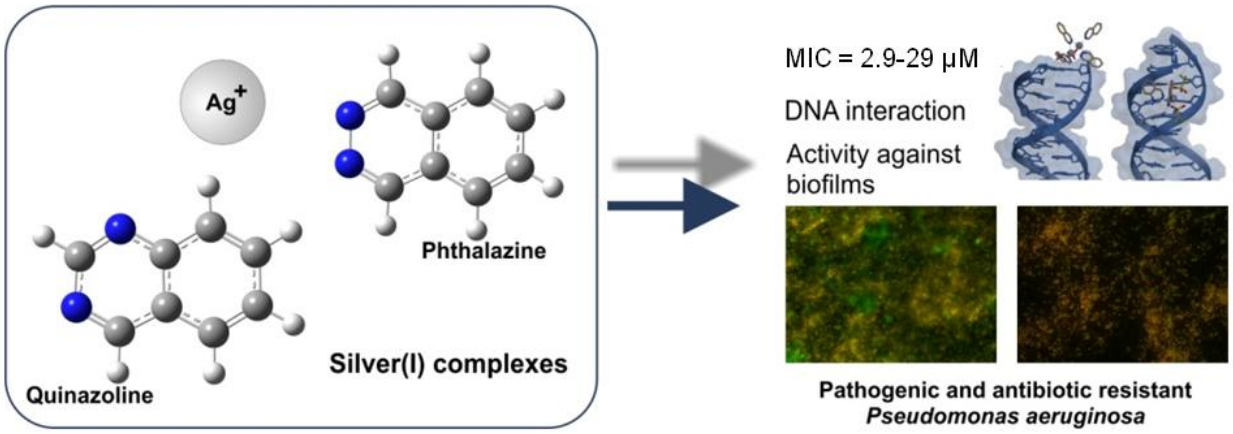

Five new silver(I) complexes with aromatic *N*-heterocycles phthalazine and quinazoline show potent activity against pathogenic *Pseudomonas aeruginosa* and can be used to prevent infections due to *P. aeruginosa* biofilms.

Research Highlights (Ms. No. JIB-15-0901)

- Synthesis and characterization of silver(I) complexes with phthalazine and quinazoline.
- Biological activities of the silver(I) complexes.
- High activity of the silver(I) complexes against *Pseudomonas aeruginosa* strains.
- Binding of the silver(I) complexes to genomic DNA from *Pseudomonas aeruginosa.*